Imaging of Vertebral Artery Dissection in Children: An Underrecognized Condition with High Risk of Recurrent Stroke

Stephen B. Little, MD • Asha Sarma, MD* • Manish Bajaj, MD • Sumit Pruthi, MBBS • Kartik Reddy, MD • Andrew Reisner, MD*
Bryan Philbrook, MD • Lori C. Jordan, MD, PhD

*S.B.L. and A.S. contributed equally to this work.
Author affiliations, funding, and conflicts of interest are listed at the end of this article.

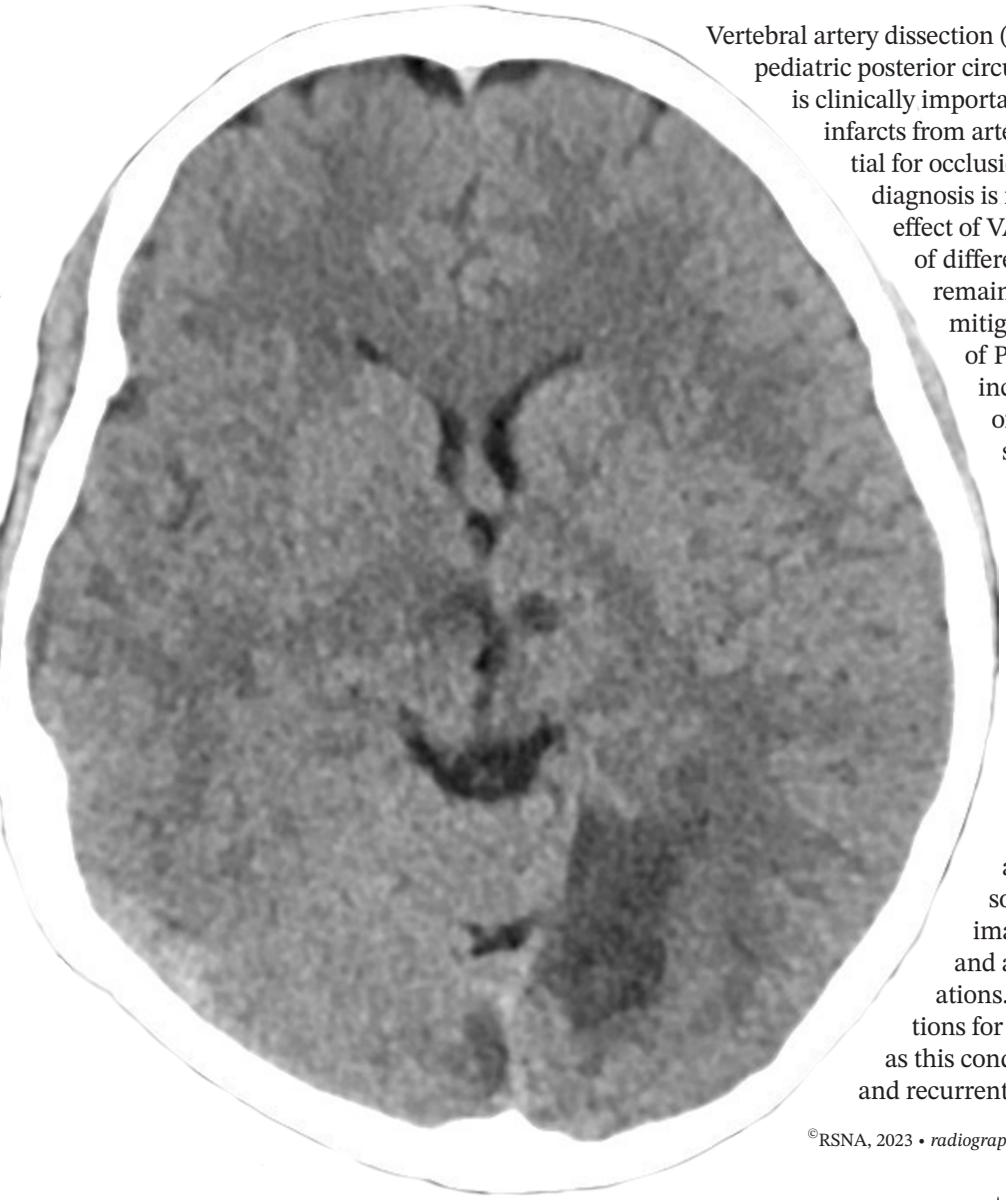

Vertebral artery dissection (VAD) is a common cause of a rare condition, pediatric posterior circulation arterial ischemic stroke (PCAIS). VAD is clinically important due to the risk of multifocal and continuing infarcts from artery-to-artery thromboembolism, with the potential for occlusion of arteries that perfuse the brainstem. Early diagnosis is important, as recurrent stroke is a common effect of VAD in children. Although the relative efficacies of different treatment regimens for VAD in children remain unsettled, early initiation of treatment can mitigate the risk of delayed stroke. Clinical diagnosis of PCAIS may be delayed due to multiple factors, including nonspecific symptoms and the inability of younger patients to express symptoms. In fact, subacute or chronic infarcts are often present at initial imaging. Although the most common cause of isolated PCAIS is VAD, imaging of the cervical arteries has been historically underused in this setting. Cervical vascular imaging (MR angiography, CT angiography, and digital subtraction angiography) for VAD must be optimized to detect the sometimes subtle findings, which may be identified at initial or follow-up imaging. Osseous variants of the craniocervical junction and upper cervical spine and other extrinsic lesions that may directly injure the vertebral arteries or lead to altered biomechanics have been implicated in some cases. The authors review characteristic imaging features and optimized imaging of VAD and associated PCAIS and related clinical considerations. Identification of VAD has important implications for evaluation, treatment, and imaging follow-up, as this condition may result in progressive arteriopathy and recurrent stroke.

Supplemental Material

Quiz questions for this article available through the Online Learning Center.

RadioGraphics 2023; 43(12):e230107
https://doi.org/10.1148/rg.230107

Content Codes: NR, PD, VA

Abbreviations: CASCADE = childhood AIS standardized classification and diagnostic evaluation, MIP = maximum intensity projection, PCAIS = posterior circulation arterial ischemic stroke, 3D = three dimensional, TOF = time of flight, TSE = turbo spin echo, 2D = two dimensional, VAD = vertebral artery dissection

TEACHING POINTS

- Multifocal isolated PCAIS lesions (due to vessel-to-vessel thromboembolism) and strokes of varying age seen at initial imaging are highly suggestive of VAD. In some cases, only chronic infarcts are seen at the time of initial imaging.
- Intracranial MR or CT angiograms may reveal abrupt posterior circulation arterial occlusions due to vessel-to-vessel thromboembolism. These occlusions are highly suggestive of VAD as the underlying cause and, if present, should prompt cervical vascular imaging.
- Most VADs in children occur at the C2 level and typically involve the horizontal proximal V3 segment or adjoining V2-V3 segment junction. The V3 segment may be particularly vulnerable to repetitive microtrauma owing to its proximity to the lateral aspect of the mobile atlantoaxial joint.
- Compared with carotid artery dissection, VAD presents unique neuroimaging challenges. Anatomic features that mandate a different approach include surrounding bone, generally smaller artery size, tortuosity of the V3 segment, and the periarterial venous plexus.
- Cervical arterial dissection, especially posterior circulation dissection, can change over time. Nearly 50% of vessel abnormalities progress within the first year, and some arterial abnormalities may be detected only at follow-up.

Introduction

Posterior circulation arterial ischemic stroke (PCAIS) represents approximately 15%–22% of cases of childhood arterial ischemic stroke and is believed to be underdiagnosed due to variable and nonspecific clinical presentations (1). The cause of PCAIS is often never determined (2). Although the outcomes of patients with PCAIS are better overall than the outcomes of those with anterior circulation arterial ischemic stroke, recurrent infarction is 6.4 times more common. Thus, timely diagnosis and treatment are vital (1,3). Children with intrinsic arteriopathy, including VAD, are five times more likely to experience recurrent arterial ischemic stroke than children with an extrinsic etiology (eg, thromboembolism), and they may have worse outcomes (Fig 1) (4,5). These data differ from those for adults, which indicate that recurrent carotid or vertebral stroke 12 months after cervical artery dissection is uncommon (1%–2%) (6).

Vertebral artery dissection (VAD) is the most common cause of isolated PCAIS and has been implicated in up to 44%–50% of pediatric cases. However, the actual contribution of VAD to isolated PCAIS is probably greater owing to heterogeneous imaging workups, challenges related to poor image quality, and lack of consensus in classifying cerebral arteriopathies, even among experts (2,5,7,8). In patients with PCAIS, the imaging findings of VAD, even when they are recognizable in retrospect, are frequently missed at initial review, even at institutions that have clinicians with high levels of expertise. Cervical arterial imaging and follow-up imaging are underused (5,9,10). PCAIS has been associated with errors in the initially suspected diagnosis in 55% of cases, compared with in 20% of cases in the setting of anterior circulation arterial ischemic stroke (11). As many as 50%–60% of cases of PCAIS may be misclassified with MR angiography, and the value of CT angiography for diagnosis of VAD in children has not been well studied (2,12,13).

These issues have prompted the American Heart Association to recommend development of better imaging techniques for early and accurate diagnosis of VAD (14). Accurate timely diagnosis of pediatric VAD is important for secondary stroke prevention; British and Australian clinical guidelines for VAD recommend anticoagulation rather than aspirin, which is recommended for other arteriopathies (2,15). The American Heart Association guideline is equivocal in terms of whether aspirin or anticoagulation is preferred for secondary stroke prevention after VAD in children and adults (14,16).

In this article, we share our experiences in imaging pediatric VAD to improve the care of children with PCAIS. Topics reviewed include *(a)* key clinical considerations, *(b)* relevant anatomy, *(c)* practical strategies to optimize imaging, *(d)* key imaging findings of pediatric VAD, and *(e)* significance of osseous variants and the role of dynamic rotational angiography.

Clinical Considerations in Patients with VAD and PCAIS

Risk Factors, Etiopathogenesis, and Clinical Presentation

Risk factors for craniocervical arterial dissection in children include male sex, head and neck trauma, and possibly connective tissue disorders leading to vessel wall structural differences (9,17,18).

VAD is caused by tearing or separation of the tunica intima (9). PCAIS involves multiple infarct locations in 39.5% of cases. Infarcts of varying age are common with extradural VAD, suggesting vessel-to-vessel thromboembolism from the injured artery as the underlying cause (19,20). While lateral medullary infarcts are more common in adults, cerebellar and thalamic infarcts are more common in children (21).

Since many brain structures can be injured in PCAIS, the presenting symptoms are highly variable. These may include headache, vertigo, speech disturbance, hemiparesis, altered consciousness, vision change, ataxia, emesis, and seizure (1,20,22,23). Communication difficulties in young patients and often-nonspecific clinical presentations may result in difficult and sometimes delayed recognition of PCAIS (23). Identification of underlying VAD at neuroimaging is also frequently delayed. In their study involving 20 children, Simonnet et al (21) described a mean delay of 22 days between symptom onset and imaging diagnosis of VAD. Delays may, in part, occur because the imaging findings of VAD are often first recognized at follow-up imaging (2,14).

In previous studies, many patients with PCAIS did not undergo cervical arterial imaging despite the high association of PCAIS with VAD (9). Vertebrobasilar dissection is

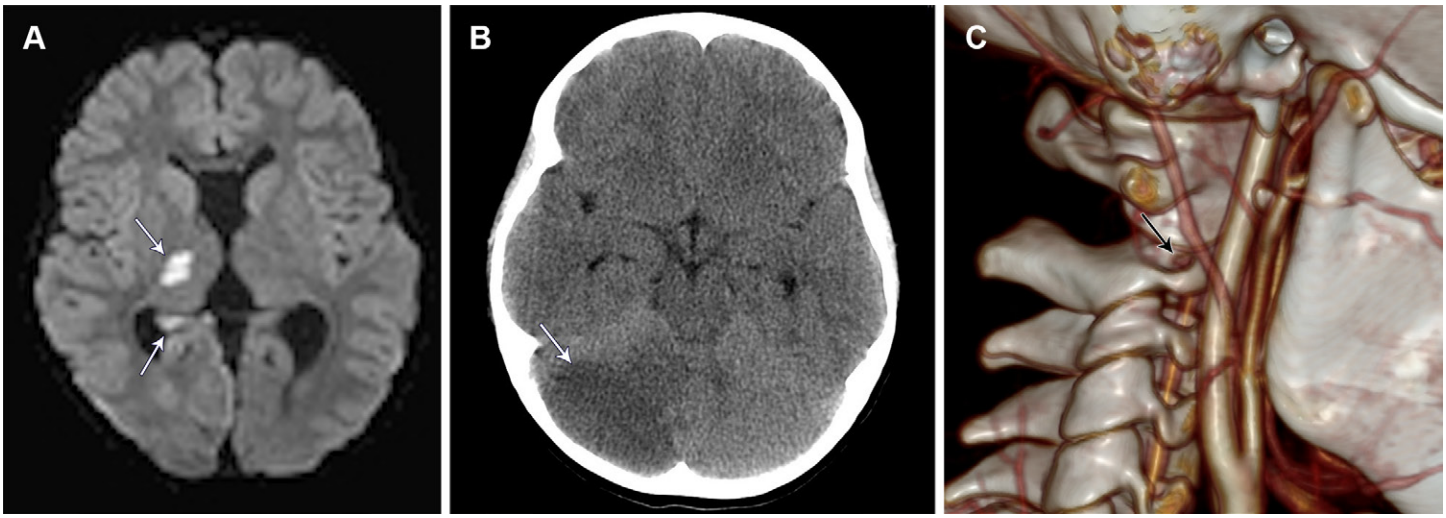

Figure 1. Recurrent stroke due to VAD in a 6-year-old girl. **(A)** Axial diffusion-weighted MR image obtained the day of presentation (day 0) shows acute infarcts (arrows) in the right thalamus and hippocampal tail. **(B)** Axial CT image on day 6 after presentation shows a new right cerebellar infarction (arrow) that was not present on day 0. **(C)** Right lateral volume-rendered CT image shows vertebral artery occlusion (arrow).

more common than carotid dissection in children and is the most common cause of isolated PCAIS (2,3,24). Although cervical arterial imaging for suspected VAD is frequently prompted by trauma (eg, from a motor vehicle collision or spinal injuries), a history of trauma may be absent in nearly half of cases of pediatric cervical arterial dissection (5,9,25). In addition, the reported trauma may seem innocuous (eg, from contact sports, physical exertion, neck manipulation, or neck hyperextension) (14).

Indications for Imaging

Imaging of the vertebral arteries is required in children with an acute focal neurologic deficit, stroke, or transient ischemic attack that can be localized to the posterior circulation. In more than 50% of children with stroke due to arterial dissection, a headache is also reported (17). CT angiography or MR angiography to evaluate for cervical arterial injury is recommended for children with cervical spine traumatic injuries, including fractures involving the transverse foramina; facet fracture and/or dislocation; ligamentous injury; and fractures involving the C1 through C3 vertebral bodies. Adult scoring systems that are used to determine which patients with blunt spinal trauma should undergo vascular imaging have not yet been validated in children (26).

Treatment Considerations

Pediatric VAD is clinically important owing to the associated high risks of recurrent stroke, progressive vascular stenosis, or brainstem artery occlusion. Even when VAD is clinically suspected, it may be difficult to identify at imaging, leaving treating physicians, children, and families uncertain about the diagnosis, treatment, activity restrictions, and timing of serial imaging.

At least theoretically, anticoagulation (eg, low–molecular-weight heparin or warfarin) should provide better protection against stroke recurrence than antiplatelet therapy. However, adult trials have been inconclusive. In the CADISS (Cervical Artery Dissection in Stroke Study) trial (6), which included 250 randomly selected adults with cervical artery dissection and stroke, 2% of patients (four in the antiplatelet arm, two in the anticoagulation arm) had recurrent strokes during a 12-month follow-up period; the difference in outcomes between the two treatment groups was not statistically significant. In contrast, in the TREAT-CAD trial (27) involving 173 adults with cervical dissection, seven of 91 patients (8%) in the aspirin group and no patients in the vitamin K antagonist group had recurrent ischemic strokes; thus, noninferiority of aspirin was not shown. Larger trials of cervical artery dissection and stroke in adults are not considered to be feasible and thus are even less likely to be performed in children. Treating physicians balance the risks of anticoagulation versus aspirin when the benefit is unclear, leading to individualized decisions.

VAD with pseudoaneurysm is significantly more likely to be associated with recurrent infarction despite the initiation of anticoagulation or antiplatelet therapy at the time of initial diagnosis (22). Patients with a pseudoaneurysm that is suspected to be related to rotational vertebral artery injury and recurrent PCAIS despite antithrombotic therapy may be treated with a hard cervical collar or surgery (eg, cervical decompression or fusion) (22). Some authors recommend placing a neck brace for V3 (atlas loop) segment VAD until documentation of healing at 3-month follow-up MR angiography (24).

Arterial Anatomy Relevant to Pediatric Patients with PCAIS and VAD

Understanding the relevant anatomy in pediatric VAD and PCAIS is key to accurately diagnosing these entities. This anatomy is detailed herein to contextualize imaging abnormalities. Anatomic variation is common. The most common configurations are described (Fig 2) (28).

Vertebral and Basilar Arteries

The V1 (preforaminal) vertebral artery segment extends from the origin at the subclavian artery to the level of entry into the vertebral transverse foramina, usually the C6 cervical vertebra

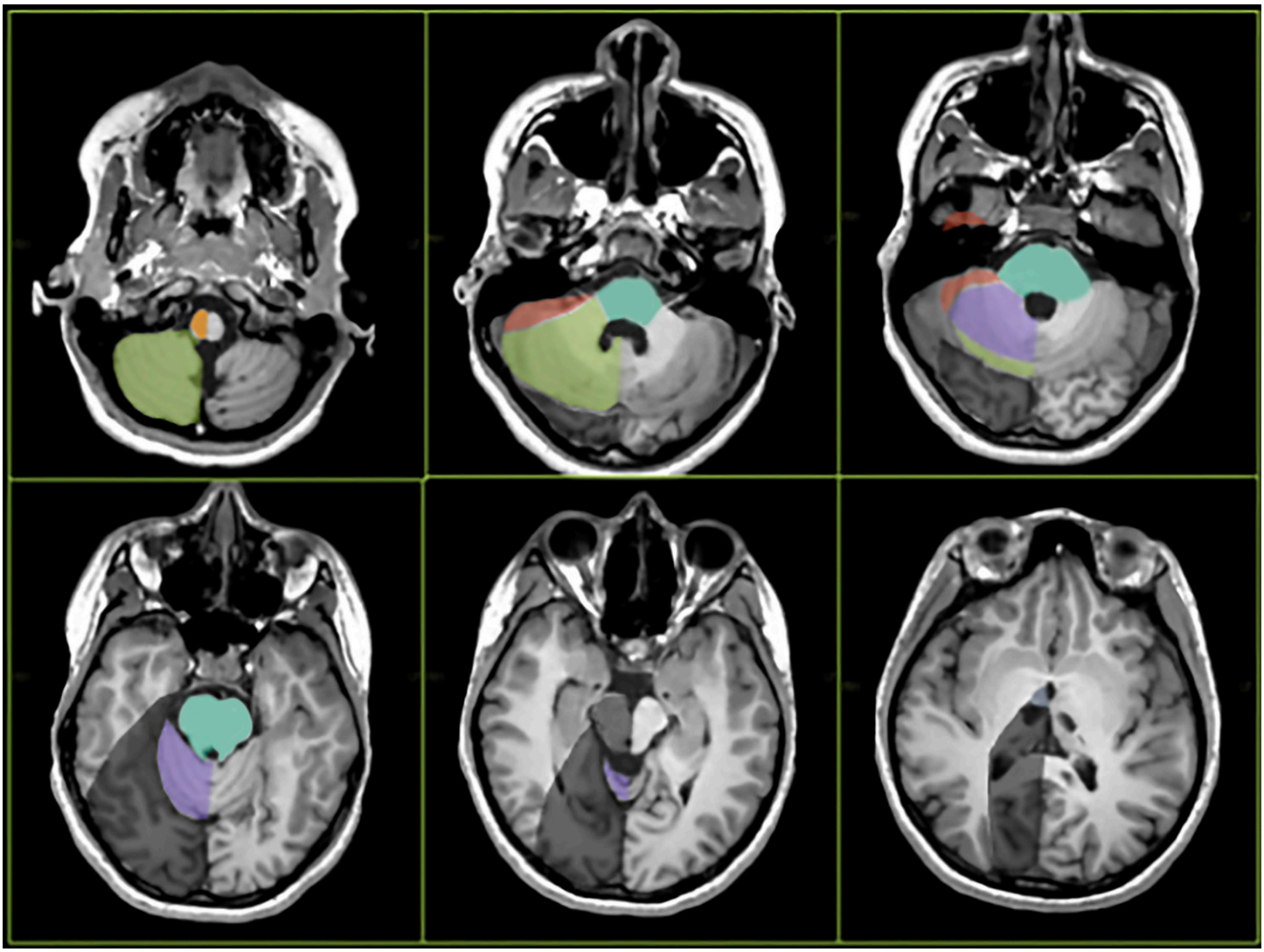

Figure 2. Axial T1-weighted MR images from inferior to superior (left to right) show the posterior circulation arterial blood flow territories. The vertebral artery territory is shaded orange; the basilar artery, teal; the posterior-inferior cerebellar artery, light green; the anterior-inferior cerebellar artery, red; the superior cerebellar artery, purple; and the posterior cerebral artery, dark gray.

(Fig 3). The V2 (foraminal) segment extends from the transverse foramen of C6 to the transverse foramen of C2. The V3 (atlantic, extradural, or extraspinal; atlantic loop) segment extends from the C2 transverse foramen to the point of entry into the intradural intracranial compartment. V4 is the intradural (or intracranial) segment. The posterior-inferior cerebellar artery usually arises from the V4 segment. The paired vertebral arteries join to form the basilar artery. The basilar artery branches include the anterior-inferior cerebellar artery, superior cerebellar artery, and posterior cerebral artery.

Posterior Cerebral Circulation

The paired posterior cerebral arteries arise from the basilar artery and anastomose with the anterior circulation through the posterior communicating arteries to form the circle of Willis. The P1 posterior cerebral artery segment extends from the basilar artery origin to the origin of the posterior communicating arteries. Thalamoperforator arteries arise from P1 and supply the midbrain and thalamus. The P2, P3, and cortical branches of the posterior cerebral artery supply the thalamus, inferomedial temporal lobe, hippocampus, occipital pole, visual cortex, and callosal splenium, explaining the wide variety of potential PCAIS locations (Fig S1).

Cerebellar Arterial Supply

The posterior-inferior cerebellar artery supplies the ipsilateral vermis and cerebellar hemisphere below the horizontal fissure. The anterior-inferior cerebellar artery supplies the anteroinferior cerebellar hemisphere and middle cerebellar peduncle. The superior cerebellar artery supplies the superior vermis and cerebellar hemisphere above the horizontal fissure, dentate nucleus, and cerebellar white matter.

Brainstem Arterial Supply

The medulla is supplied by distal vertebral artery branches, the posterior-inferior cerebellar artery, and the anterior spinal artery. The pons is supplied by the superior cerebellar artery and basilar artery. The midbrain is supplied by perforators arising from the basilar, superior cerebellar, and posterior cerebral arteries.

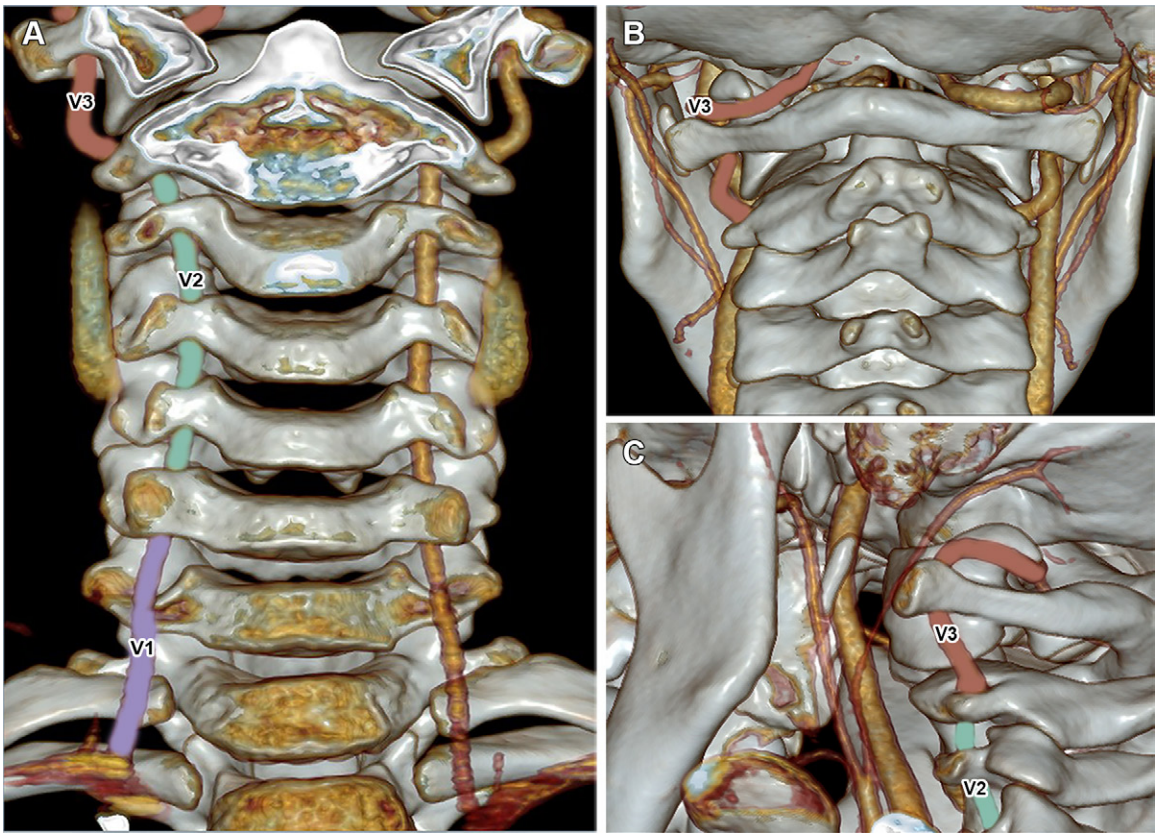

Figure 3. Volume-rendered CT angiograms show the most common configuration of normal vertebral artery anatomy. Coronal image with anterior view **(A)**, coronal image with posterior view **(B)**, and sagittal oblique view from the patient's left side **(C)** are shown. The V1, or preforaminal segment (purple), extends from the origin to the transverse foramen of C6. The V2, or foraminal segment (teal), extends from the transverse foramen of C6 to the transverse foramen of C2. The V3, or atlantic, extradural, or extraspinal segment (red), starts from C2, where the artery loops and turns laterally to ascend into the transverse foramen and continues through the C1 transverse foramen to enter the dura. The V4, or intradural segment, is not shown.

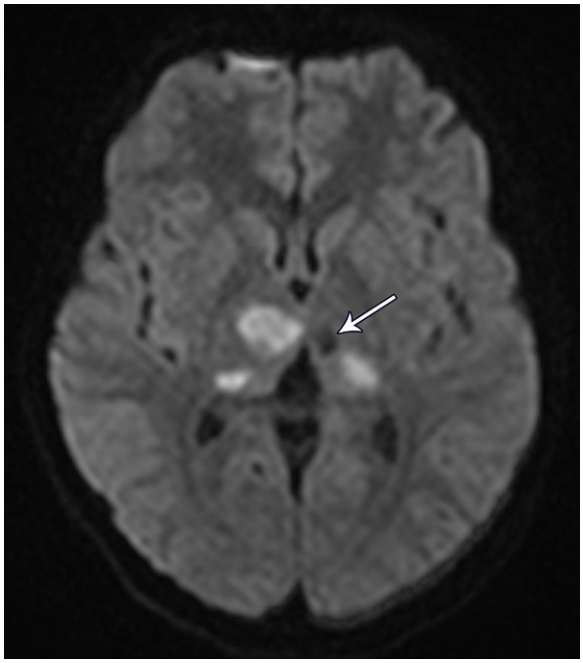

Figure 4. Infarcts of varying ages due to VAD in a 12-year-old girl. Axial diffusion-weighted MR image shows acute infarcts within both thalami, with low diffusivity confirmed on apparent diffusion coefficient maps (not shown). A chronic lacunar left thalamic infarct (arrow) does not show low diffusivity. Infarcts of different ages seen at initial imaging are common in VAD.

Intracranial Imaging Findings in Pediatric Patients with PCAIS and VAD

Multifocal isolated PCAIS lesions (due to vessel-to-vessel thromboembolism) and strokes of varying age seen at initial imaging are highly suggestive of VAD (Fig 4) (14). In some cases, only chronic infarcts are seen at the time of initial imaging. The most common locations of PCAIS due to VAD are the cerebellum, thalami, and occipital lobes (Fig 5).

Noncontrast Head CT Findings

Established infarcts are often already visible at initial CT because they may have been clinically silent at the time of acute occurrence due to nonspecific symptoms and delayed presentation (Fig 6). More subtle acute infarcts may be present as well. A hyperattenuating intravascular clot (Fig S2) is occasionally seen, sometimes as the only finding; however, partial volume averaging, beam hardening, and photon starvation artifacts limit the value of this sign.

Brain MRI

Brain MRI may show variable signal intensity characteristics of multifocal infarcts due to varying age (eg, combinations of acute infarcts with low diffusivity and chronic infarcts with increased diffusivity, and corresponding signal intensity abnormalities on T2-weighted and T2-weighted fluid-attenuated inversion-recovery images).

Intracranial MR or CT angiograms may reveal abrupt posterior circulation arterial occlusions due to vessel-to-vessel thromboembolism. These occlusions are highly suggestive of VAD as the underlying cause and, if present, should prompt

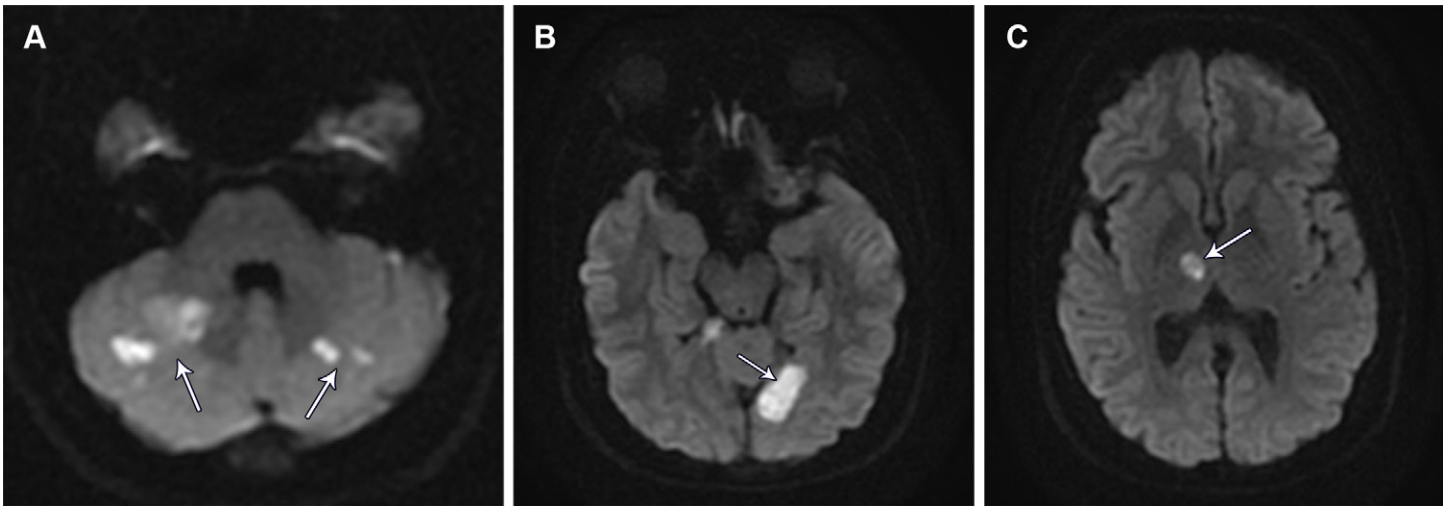

Figure 5. Multifocal posterior circulation infarcts due to VAD in a 17-year-old adolescent girl with DiGeorge syndrome, dizzy spells, paresthesias, and vomiting. Axial diffusion-weighted MR images from inferior to superior show multiple cerebellar **(A),** left occipital lobe **(B),** and right thalamic **(C)** infarcts (arrows). Multifocal isolated posterior circulation infarctions are highly suggestive of VAD.

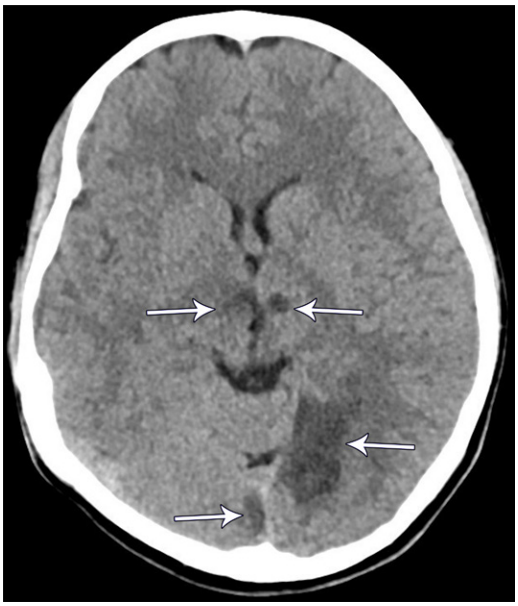

Figure 6. Multiple infarcts in a 12-year-old girl who presented with visual disturbance and numbness in the face and tongue. In VAD, established infarcts are often visible on the initial CT images due to nonspecific symptoms and delayed presentation. Axial noncontrast CT image shows areas of hypoattenuation (arrows) within both thalami and occipital lobes, consistent with subacute to chronic infarcts.

cervical vascular imaging (Fig 7). Multifocal arterial stenosis or occlusion at follow-up imaging may be due to additional vessel-to-vessel thromboembolism and/or partial recanalization of the thrombus (Fig 8), although this can be difficult to distinguish from cerebral arteriopathy (19).

Extracranial Imaging Findings in Pediatric Patients with PCAIS and VAD

The CASCADE (*c*hildhood *A*IS [arterial ischemic stroke] *s*tandardized *c*lassification *a*nd *d*iagnostic *e*valuation) classification system, developed by the International Pediatric Stroke Study Working Group, is a structured tool used for classifying childhood strokes according to the anatomic site of the underlying disease (5,29) and includes clinical and imaging features. The CASCADE imaging features relevant to VAD are summarized in Table 1 and detailed subsequently. CASCADE criteria for VAD require confirmation of the diagnosis (when possible) with CT angiography, MR angiography, or digital subtraction angiography (8).

Imaging findings of VAD are variable and can be subtle. The most important factor in recognizing VAD is the typical location of arterial injury. Most VADs in children occur at the C2 level and typically involve the horizontal proximal V3 segment or adjoining V2-V3 segment junction (Fig 9) (21,22). The V3 segment may be particularly vulnerable to repetitive microtrauma owing to its proximity to the lateral aspect of the mobile atlantoaxial joint (21,30). Distal V3 dissections are much less frequent, and the pathogenesis may be different. V1 and proximal V2 dissections are uncommon in children. Children with V3 segment VAD appear to be predisposed to recurrent stroke, even when they are receiving antithrombotic therapy (22,31). Various imaging findings have been described and include asymmetric focal stenosis, focal fusiform or blister-like dilatation, and flame-shaped vascular or tapering arterial occlusion (ie, "string" sign) in the typical locations (7,21). Findings of VAD may resolve or progress to occlusion at follow-up imaging (2,10,14,29). It is important to note that pseudoaneurysm may be first seen at initial imaging or at follow-up.

Intradural VAD may extend into the basilar artery (vertebrobasilar dissection). If transmural dissection occurs adjacent to a venous plexus (eg, the vertebral venous plexus), the patient may develop an arteriovenous fistula. Rupture into the soft tissues may lead to arterial compression (20).

CASCADE Criteria for VAD

Eccentric Mural Thickening.—Eccentric mural thickening of the vertebral artery may be seen on thin (<1-mm) sagittal

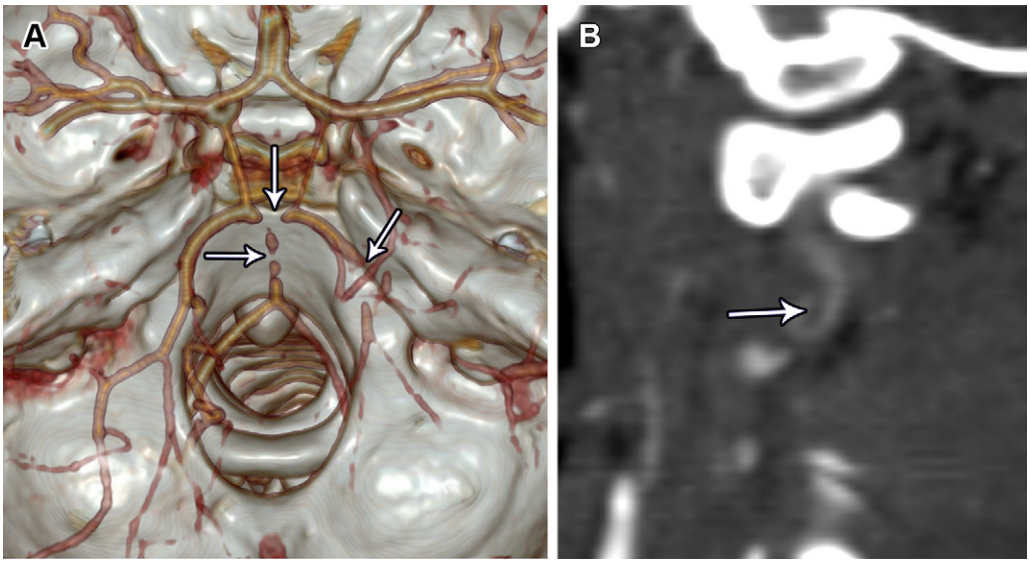

Figure 7. Posterior circulation arterial occlusions and VAD in a 6-year-old girl with left-sided weakness and facial sensory changes. **(A)** Superior volume-rendered CT angiogram shows abrupt and multifocal occlusions (arrows) of the basilar and right posterior cerebral arteries. **(B)** Sagittal multiplanar reformation CT angiogram shows segmental stenosis of the right vertebral artery at the proximal V3 level, with a possible intimal flap (arrow). Abrupt posterior circulation arterial occlusions suggest thromboembolism (usually vessel-to-vessel) and should prompt a search for VAD at cervical vascular imaging.

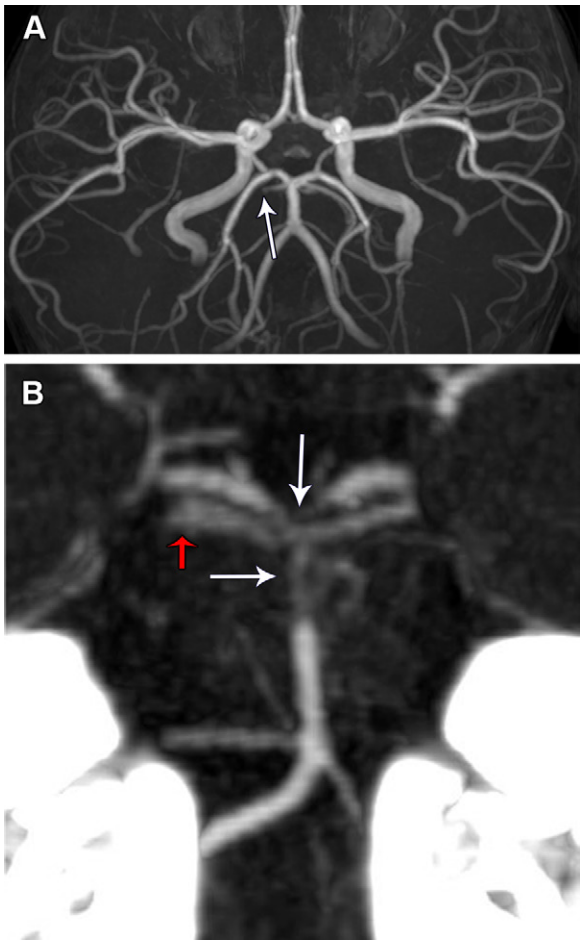

Figure 8. Progressive intracranial arterial occlusive disease due to VAD in a 3-year-old boy with weakness, ataxia, and vomiting. **(A)** Axial oblique maximum intensity projection (MIP) three-dimensional (3D) time-of-flight (TOF) MR angiogram on day 1 after presentation shows an abrupt occlusion (arrow) of the right superior cerebellar artery. **(B)** Follow-up coronal MIP CT angiogram on day 6 shows worsening multifocal stenosis and occlusion (white arrows) due to additional vessel-to-vessel thromboembolism and partially recanalized thrombus (red arrow) in the superior cerebellar artery. This finding may be difficult to differentiate from cerebral arteriopathy.

Table 1: CASCADE Criteria for Imaging-based Diagnosis of VAD

Confirmation of the diagnosis of intracranial or cervical arterial dissection requires CT angiography, MRI or MR angiography, or conventional angiography with one of the following three patterns:
1. Angiographic findings of a double lumen, intimal flap, or pseudoaneurysm, or a "crescent" sign (eg, bright signal in the arterial wall on axial T1-weighted fat-saturated MR images)
2. Clinical events including cervical or cranial trauma, neck pain, or head pain less than 6 weeks prior to angiographic findings of segmental arterial stenosis (or occlusion) in the cervical arteries
3. Angiographic stenosis (or occlusion) of the vertebral artery segment at the level of the C2 vertebral body, even without a history of trauma

Note.—Data are based on the CASCADE criteria for classification of acute primary childhood arterial ischemic stroke (Anatomic Features, Section 4 [Aortic/Cervical Arteriopathy: Definition]), developed by pediatric stroke specialists from the International Pediatric Stroke Study. (Adapted and reprinted, with permission, from reference 8.)

or coronal reformatted CT angiograms or three-dimensional (3D) time-of-flight (TOF) MR angiograms (Fig 10) (8). Thickening most commonly involves the anterior wall of the proximal horizontal V3 segment in close proximity to the lateral atlantoaxial joint. This finding is believed to represent mural hematoma and corresponds to the bright crescent sign seen on axial T1-weighted fat-saturated MR images (CASCADE section 4: a1) (8).

Pseudoaneurysms and Intimal Flaps.—Pseudoaneurysms (CASCADE section 4: a1) (8) are rarely reported in the pediatric literature, but they may be more common than previously believed. They may be more common in younger patients and almost always involve the proximal V3 segment immediately

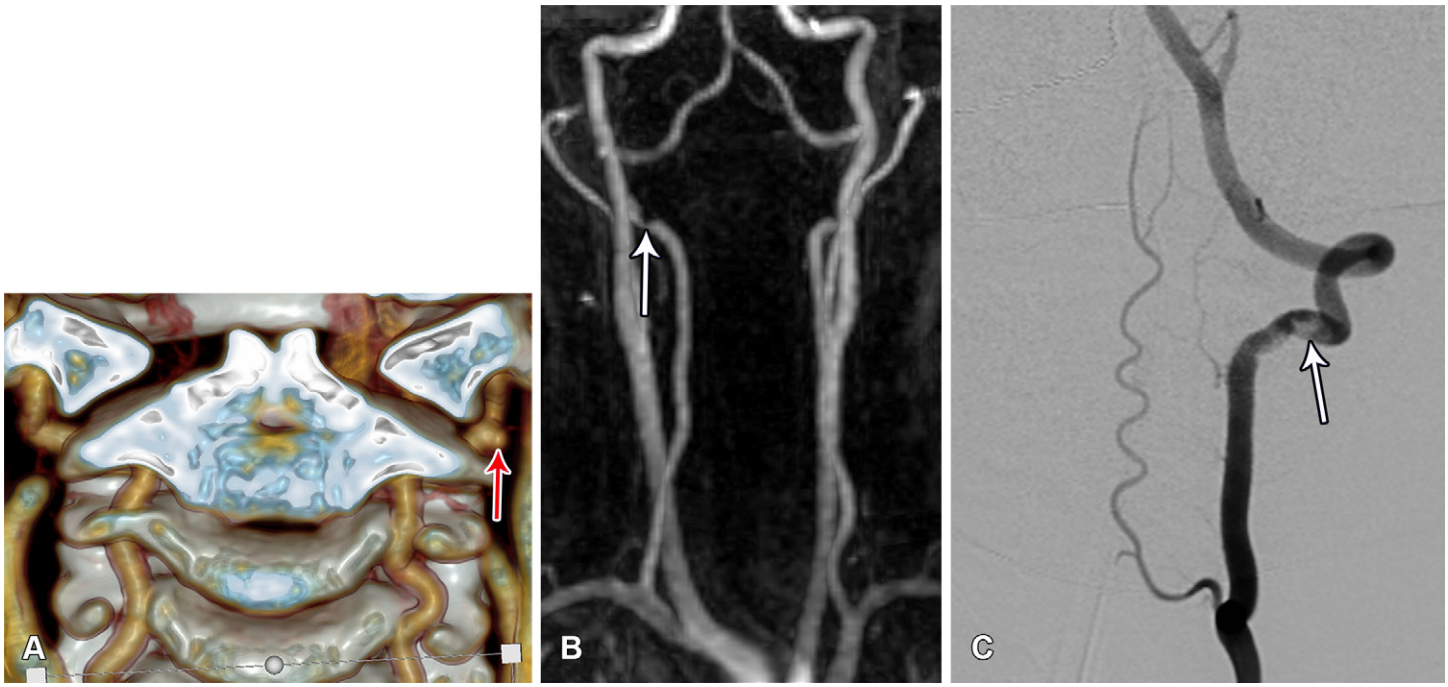

Figure 9. VAD in three children. Most VADs in children occur at the C2 level, particularly involving the V2-V3 segment junction or proximal horizontal V3 segment, possibly owing to repetitive microtrauma associated with the mobile lateral atlantoaxial joint. **(A)** Coronal volume-rendered CT angiogram in a 3-year-old boy shows a saccular pseudoaneurysm (arrow) at the V2-V3 junction. **(B)** Coronal 3D TOF MR angiogram in a 7-year-old boy shows eccentric mural thrombus (arrow) at the right V2-V3 junction. **(C)** Anteroposterior digital subtraction angiogram in a 21-month-old girl shows a filling defect (arrow) within the proximal V3 segment, consistent with VAD.

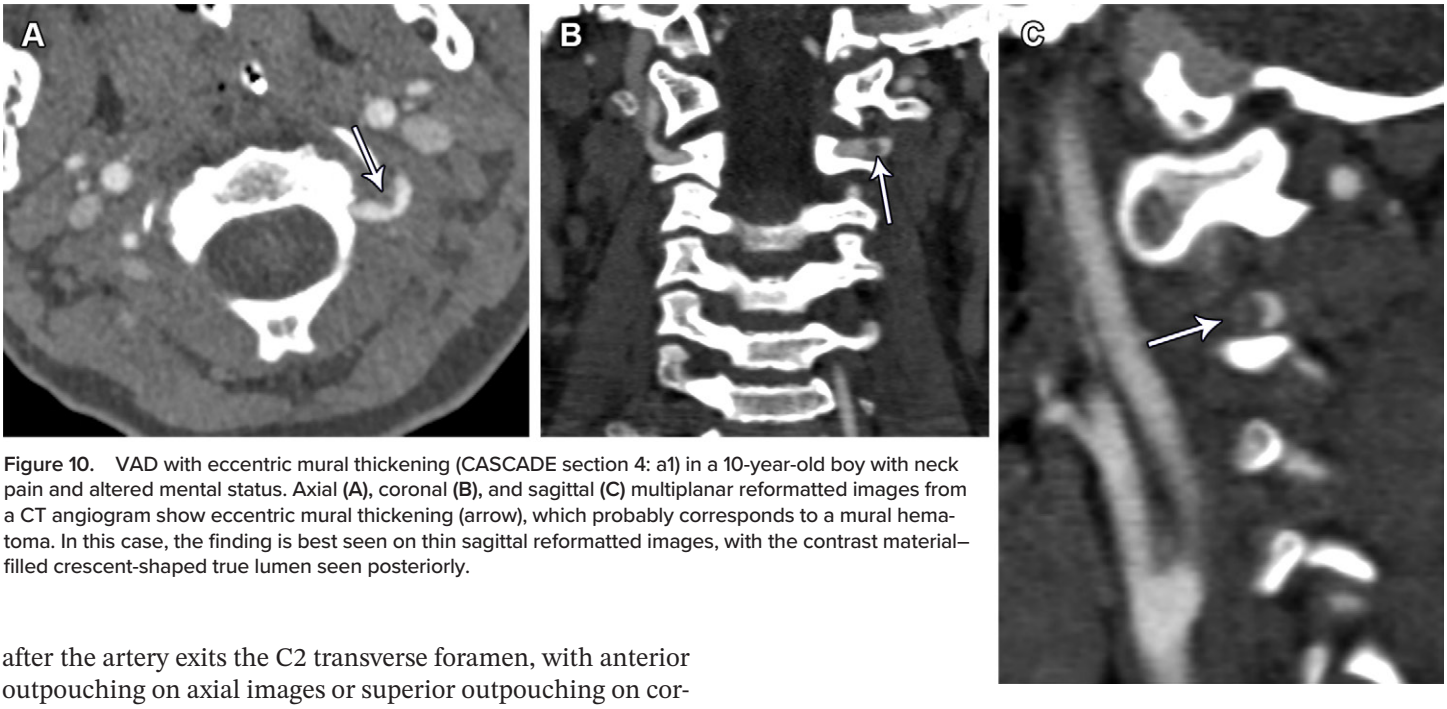

Figure 10. VAD with eccentric mural thickening (CASCADE section 4: a1) in a 10-year-old boy with neck pain and altered mental status. Axial **(A),** coronal **(B),** and sagittal **(C)** multiplanar reformatted images from a CT angiogram show eccentric mural thickening (arrow), which probably corresponds to a mural hematoma. In this case, the finding is best seen on thin sagittal reformatted images, with the contrast material–filled crescent-shaped true lumen seen posteriorly.

after the artery exits the C2 transverse foramen, with anterior outpouching on axial images or superior outpouching on coronal images (Fig 11) (22).

Despite a common misconception, intimal flaps (CASCADE section 4: a1) (8) are uncommonly seen in childhood VAD (8,32). When present, they are best seen on submillimeter 3D TOF MR angiographic source images or CT angiographic source images (Fig 12). The angiographic double lumen is very rare in pediatric VAD.

Segmental arterial stenosis or occlusion at the level of the C2 vertebral body, corresponding to the V2-V3 junction and/or proximal V3 segment, is a frequent finding in pediatric VAD, even without a history of trauma (CASCADE section 4: a3) (8). It can be easily missed on two-dimensional (2D) TOF MR angiograms due to stair-step and in-plane flow artifacts and may be better visualized with CT angiography, contrast-enhanced MR angiography (Fig 13), or digital subtraction angiography. According to the CASCADE criteria, segmental arterial stenosis (or occlusion) seen in other less commonly involved portions of

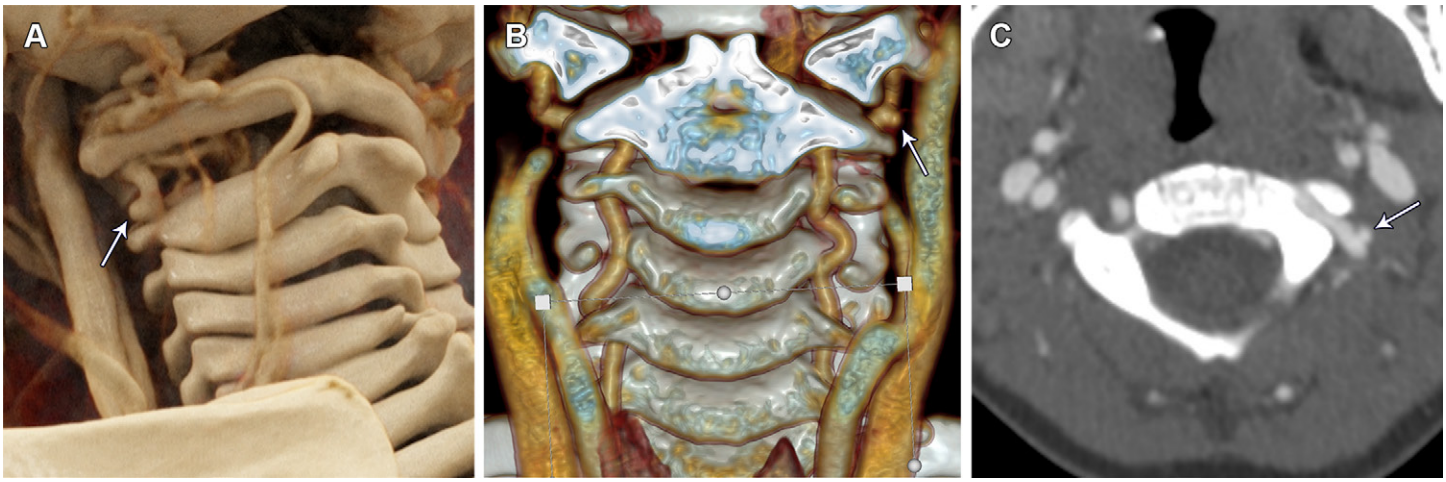

Figure 11. VAD with pseudoaneurysm (CASCADE section 4: a1) in a 3-year-old boy with nausea, vomiting, and ataxia. Left posterior oblique volume-rendered cinematic **(A)**, coronal volume-rendered **(B)**, and axial **(C)** CT angiograms show an outpouching from the left proximal V3 vertebral artery segment (arrow), representing a pseudoaneurysm. Pseudoaneurysms are more common than intimal flaps and may be seen at the time of initial imaging or at follow-up.

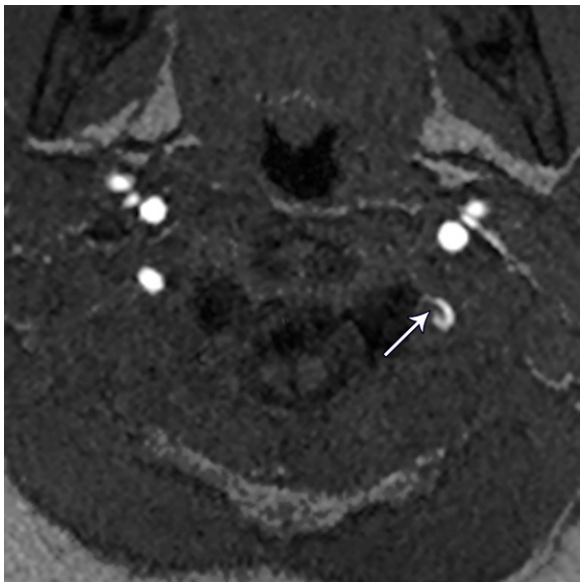

Figure 12. VAD with an intimal flap in a 14-month-old boy with vomiting, ataxia, and lethargy. Axial 3D TOF MR angiogram shows a linear filling defect (arrow) in the left vertebral artery, representing an intimal flap. Intimal flaps are uncommonly identified but are best seen on submillimeter source images from 3D TOF MR or CT angiograms.

the vertebral artery are also consistent with VAD but require a history of cervical or cranial trauma, neck pain, or head pain in the preceding 6 weeks (CASCADE section 4: a2) (8).

Strategies for Optimized Imaging of Pediatric PCAIS and VAD

Tailored, detailed, and often multimodality imaging strategies are frequently required for optimal detection and characterization of pediatric VAD and resultant PCAIS. Compared with carotid artery dissection, VAD presents unique neuroimaging challenges. Anatomic features that mandate a different approach include surrounding bone, generally smaller artery size, tortuosity of the V3 segment, and the periarterial venous plexus. Selected technical considerations are summarized in Table 2.

Head CT

Noncontrast head CT is frequently the first imaging study performed in patients with PCAIS because it is widely available and usually can be performed rapidly without sedation. Although CT is less sensitive for acute stroke than is MRI, it is frequently useful in detecting intracranial hemorrhage or other treatable disease processes (33). In addition, established PCAIS is frequently visible on CT scans. This modality is used judiciously in children to minimize the ionizing radiation dose.

CT Angiography

Head and neck CT angiography is useful for urgent vascular imaging in the setting of PCAIS, particularly in conjunction with stroke protocol head CT (primarily if MRI is unavailable or contraindicated). CT angiography can depict arteriopathies, thromboembolic disease, and predisposing osseous anomalies. It has been shown to have high interrater reliability and can be used to troubleshoot cases with artifacts related to slow or turbulent flow at noncontrast MR angiography (34). Digital subtraction angiography or CT angiography has been recommended when neck MR angiography results are negative or inconclusive in a child in whom multiple strokes are visible on diffusion-weighted images (35).

The scan timing is critical when performing CT angiography for VAD in children. Late bolus timing with opacification of the periarterial venous plexus makes evaluation of the vertebral artery difficult (Fig S3). The patient-specific circulation time may be determined with intravenous injection of a contrast agent test bolus or by using automated or semiautomated triggering software (36). We generally prefer the test bolus technique, but either technique may be used if the acquired images show robust arterial enhancement and little or no venous contamination.

Dynamic CT angiography with patient head-turning maneuvers is sometimes used to detect position-dependent

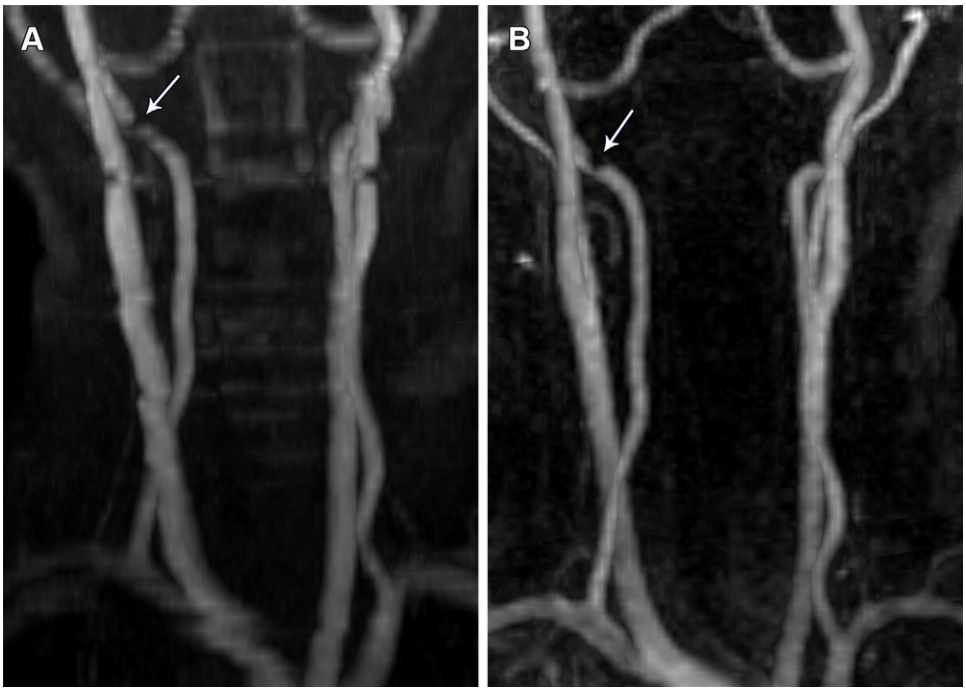

Figure 13. VAD with segmental stenosis (CASCADE section 4: a3) in a 7-year-old boy with headache, nausea, vomiting, and ataxia. Coronal 2D TOF MIP **(A)** and contrast-enhanced MIP **(B)** MR angiograms show eccentric segmental stenosis (arrow) of the right proximal V3 vertebral artery segment. Patient motion and stair-step artifacts make this finding difficult to visualize at nonenhanced imaging **(A)**; it is visualized more clearly at contrast-enhanced imaging **(B)**.

arterial compression and impingement. However, this is not performed in the acute setting because of the risk of worsening the dissection (31,37).

Use of newer CT technologies improves visualization of the vertebral arteries. Dual-energy (or photon-counting) CT may yield low–photon-energy virtual monoenergetic reconstructions that increase the brightness of iodine-containing vessels so that they are better seen when the bolus timing is suboptimal (Fig 14). Virtual noncalcium ("black bone") reconstructions may help to distinguish the opacified vertebral artery from adjacent bone. Photon-counting CT will lead to improvements by decreasing beam-hardening artifacts, reducing noise, increasing spatial resolution, and further optimizing spectral imaging (38).

Reviewing thin (thickness of 1 mm or less) reformatted images in three planes is essential for interpretation of CT angiograms obtained for pediatric VAD. Eccentric mural thickening is particularly well demonstrated on thin sagittal or coronal reformatted images. Additional CT postprocessing also is often helpful. Maximum intensity projection (MIP) images are useful for depicting the intracranial arteries and may be useful for depicting the vertebral artery with high-quality bone subtraction. Volume-rendered images are particularly useful for demonstrating the relationship between abnormal arterial segments and potentially pathogenic osseous anomalies. Postprocessing tools are increasingly being built into picture archiving and communication systems and can expeditiously create reconstructions similar to those featured in this review.

Brain MRI

MRI of the brain, including diffusion-weighted imaging, is the preferred imaging modality for initial detection of acute stroke in pediatric patients owing to its much higher sensitivity (77%) as compared with that of CT (16%) within the first hours of symptom onset (39). Sedation may be avoided by using limited sequences and protocol optimization to decrease patient motion artifacts, including those seen with various fast MRI techniques such as simultaneous multisection acquisition, parallel imaging, undersampling, and radial acquisitions (40). We have found acute MRI without sedation to be feasible in about 70% of cases of suspected pediatric stroke (41).

Head and Neck MR Angiography

Intracranial MR angiography is useful for noninvasive detection of cerebral arteriopathies and may be performed in the same session as brain MRI (33). Therefore, MR angiography is the screening vascular imaging study of choice at most institutions (14). Cervical MR angiography should be performed in cases of isolated PCAIS due to the high association of isolated PCAIS with VAD, and it may be performed in the same session as initial brain MRI. Again, abrupt posterior circulation (intracranial) arterial occlusions suggest thromboembolism and should prompt cervical vascular imaging. To ensure evaluation for alternative causes of PCAIS and optimize sensitivity for VAD, z-axis coverage of neck MR angiography should extend from the vertebral artery origins to the V4 segments, overlapping with intracranial MR angiography.

Numerous technical factors affect the acquisition time length and image quality. 3.0-T MRI is preferred over 1.5-T MRI, primarily owing to the potential for shorter pulse sequence acquisition times and/or higher spatial resolution. Among other things, acquisition time and coverage depend on the pulse sequence, the number of head and neck coil elements, and certain MRI vendor-associated idiosyncrasies. Compressed sensing and parallel imaging are typically used to decrease the acquisition time. Generally, we adjust parameters to produce sequences that require less than 5–6 minutes.

Typical cervical MR angiographic pulse sequences include 3D and 2D TOF MR angiography. 3D contrast-enhanced MR

Table 2: Common Noninvasive VAD Imaging Techniques

Technique	Pearls	Pitfalls	Recommendations
Usually preferred			
3D TOF MRA	A good first choice, particularly if performed in conjunction with stroke protocol brain MRI	In-plane flow in horizontal V3 segment Intravoxel dephasing Signal intensity ambiguity: T1 hyperintense thrombus vs flow-related enhancement	For time savings, targeted 3D TOF MRA of distal V2 and V3 segments in large patients Entire neck may be imaged in small patients Consider for follow-up imaging to avoid ionizing radiation MIP images are essential for all MRA techniques
CE MRA	Complements 3D TOF MRA	Contrast agent bolus timing may be too early or late; bolus may be too small Insufficient spatial resolution	Best for imaging aortic arch and great vessel origins
CTA	A good first choice, particularly if performed in conjunction with brain CT when MRI is unavailable or contraindicated Ideal for assessing for pathogenic osseous anomalies (at initial imaging or follow-up)	Ionizing radiation Contrast agent bolus–related issues similar to those with CE MRA	Consider a test timing bolus (our preferred technique) Dual-energy examination preferred but not required Submillimeter multiplanar reformations and MIP images are very useful 3D reformations are very useful for assessment of osseous abnormalities and their relationship with VAD
Usually not preferred			
2D TOF MRA	May be useful for vertebral artery diseases other than VAD	Insufficient spatial resolution (z-axis), stair-step artifact In-plane flow artifact in horizontal V3 segment Intravoxel dephasing Signal intensity ambiguity: difficult to differentiate T1-hyperintense thrombus from flow-related enhancement	Insensitive for VAD
T1-weighted 2D TSE FS MRI		Insufficient spatial resolution (z-axis) Slow blood flow proximal or distal to obstruction, slow flow in periarterial venous plexus, and inhomogeneous fat suppression may lead to artifacts that mimic thrombus Acute mural hematoma may not be T1 hyperintense Time consuming (thin images required) Often nondiagnostic in patients with dental braces	Avoid Consider T1-weighted 3D TSE FS MRI (vessel wall imaging)
2D TSE double–inversion-recovery (black-blood) MRI	May be useful if targeted to area of interest (eg, proximal V3 segment)	Insufficient spatial resolution (z-axis) Limited number of sections per repetition time	Opt for thinner (<3 mm) sections

Note.—CE = contrast enhanced, CTA = CT angiography, FS = fat saturated, MRA = MR angiography, TSE = turbo spin echo.

angiography may be used at some sites. These MRI examinations may be supplemented by vessel wall or black blood sequences such as T1-weighted 2D turbo spin-echo (TSE) fat saturated, T1-weighted 3D TSE fat saturated, and 2D TSE double inversion recovery. Although MIP images are useful for interpreting MR angiographic findings, they may make vessels appear smaller owing to the removal of slow-flow areas at the edges (30).

3D TOF MR angiography is a good choice for initial cervical vascular imaging in the setting of PCAIS, particularly in conjunction with stroke protocol brain MRI. Pitfalls include signal intensity dropout due to in-plane flow in the horizontal V3 segments that can simulate stenosis or occlusion; intravoxel dephasing in areas with turbulent flow; lower sensitivity to slow flow; and difficulty differentiating between T1-hyperintense mural thrombus and flow-related enhancement (30). Symmetry may sometimes be a tip-off to artifact; however, the radiologist must beware of bilateral dissections (30). Artifacts from braces or dental amalgam are frequently present on TOF MR angiograms obtained in children.

Diminished flow-related enhancement due to loss of phase coherence from different flow velocities closer to and further

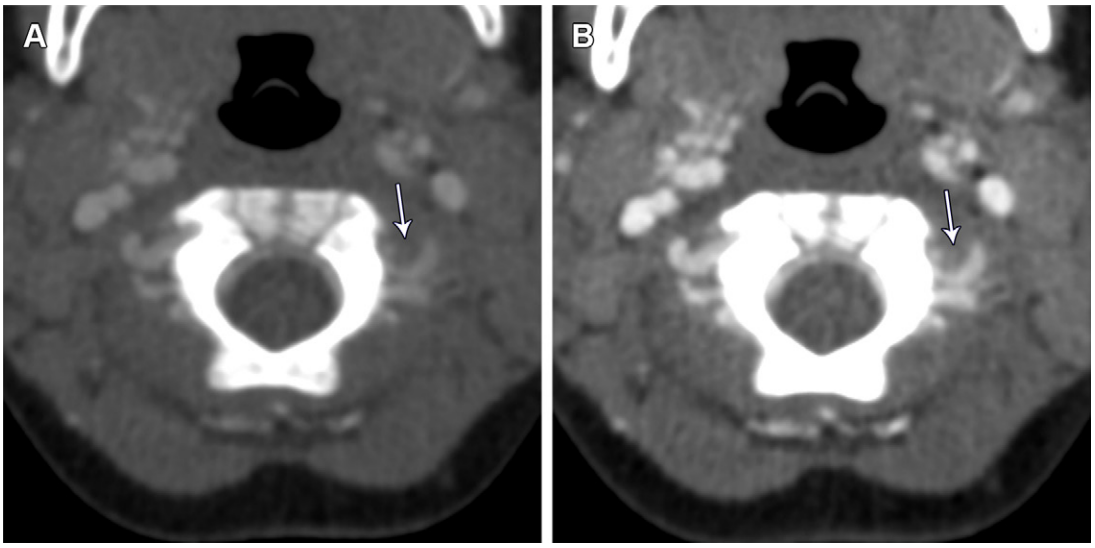

Figure 14. Left VAD in a 21-month-old girl. Low–kiloelectron-volt virtual monoenergetic reconstructions from dual-energy CT angiography may increase the conspicuity of VAD in cases of a poorly timed contrast agent bolus. **(A)** On the 70-keV virtual monoenergetic image, weak arterial enhancement and extensive venous contamination lead to poor visualization of the VAD (arrow). **(B)** On the 45-keV virtual monoenergetic reconstruction, the contrast-to-noise ratio is improved—due to an increased photoelectric effect just above the k-edge of iodine—and the conspicuity of the segmental stenosis and eccentric mural thickening of the left proximal V3 segment (arrow) is increased despite venous contamination.

from the vessel wall (which can be exacerbated by complex, high-velocity, turbulent flow) may be improved by shortening the echo time, decreasing the voxel size, and minimizing field heterogeneity (30). Submillimeter sections and near-isotropic voxels are recommended to optimize spatial resolution (13). As with angiography of the circle of Willis, 3D TOF MR angiography is well suited for evaluation of the tortuous V2-V3 junction and V3 arterial segment. An advantage of 3D TOF MR angiography, as compared with contrast-enhanced MR angiography or CT angiography, is that the vertebral arteries are not obscured by contrast material within the periarterial venous plexus.

Contrast-enhanced MR angiography is particularly well suited for imaging the aortic arch and great vessel origins and identifying cervical artery pseudoaneurysms. Thus, contrast-enhanced MR angiography of the neck is often used when there is concern for cervical artery dissection. Although the time-resolved technique is more reliable than the first-pass technique in young children who require smaller volumes of injected contrast agent, spatial resolution is sacrificed with this approach. Pitfalls of contrast-enhanced techniques include *(a)* difficulty with contrast agent bolus timing, which may lead to obscuration of the artery by the surrounding periarterial venous plexus, a notable consideration that distinguishes vertebral from carotid imaging (Fig S4); *(b)* limited allowable contrast agent volume in small patients; and *(c)* insufficient spatial resolution. Contrast-enhanced MR angiography and CT angiography may more accurately delineate the level of arterial occlusion than flow-dependent techniques if there is proximal slow flow; however, 3D TOF MR angiography typically has better spatial resolution than contrast-enhanced MR angiography and may help clarify abnormalities when there is poor contrast agent bolus timing (Fig 15). In summary, 3D TOF and contrast-enhanced MR angiographic examinations of the neck are complementary imaging studies.

2D TOF MR angiography is less desirable due to inadequate spatial resolution and frequent artifacts (30). Stair-step and in-plane flow artifacts commonly involve the proximal V3 segment, which is most often involved in pediatric VAD. Segmental stenosis is a common finding in VAD that may be easily overlooked or, more often, misattributed to "expected" stair-step and in-plane flow artifacts involving the horizontal V3 segments. In addition to the pitfalls common to all of the previously mentioned TOF techniques, z-axis (craniocaudal dimension) spatial resolution may be inadequate for visualization of VAD; the typical recommended section thickness is 2 mm. Remember that the arterial abnormality may be only a few millimeters in length (and horizontally oriented).

Intramural hematomas (visible on T1-weighted fat-saturated MR images) are frequently reported in cases of VAD; they were seen in 76%–91% of dissected vessels in studies by Oelerich et al (42), Arnold et al (43), and Vertinsky et al (44). However, nearly all of the patients in these studies were adults, and the usefulness of the crescent sign in pediatric VAD is unclear. Due to multiple potentially confounding factors, T1-weighted 2D TSE fat-saturated MRI is often of limited value despite being widely used (including in the CASCADE criteria) and being recommended in numerous publications, including the 2019 scientific statement from the American Heart Association (14): *(a)* Intraluminal hyperintense signal that may mimic thrombus may be produced by slow or turbulent blood flow, even in healthy patients (44–46). Such artifacts may be exacerbated by arterial obstruction proximal or distal to the area of interest (Fig 16A). *(b)* Slow flow in the periarterial venous plexus or inadequate fat suppression further complicates interpretation (32). *(c)* Acute mural hematoma may not be T1 hyperintense (44,45). *(d)* Many pediatric patients have dental amalgam or orthodontic hardware that causes poor-quality images due to geometric distortion, susceptibility artifacts, and inadequate fat suppression.

T1-weighted 3D TSE fat-saturated (vessel wall) MRI provides more reliable suppression of intraluminal signal than does T1-weighted 2D TSE fat-saturated imaging. Furthermore, isotropic acquisition allows multiplanar reconstruction (45,47). Alternatively, McNally et al (48) demonstrated significantly higher interrater reliability in detection of intramural hematoma with a heavily T1-weighted 3D magnetization-prepared rapid gradient-echo sequence, as compared with

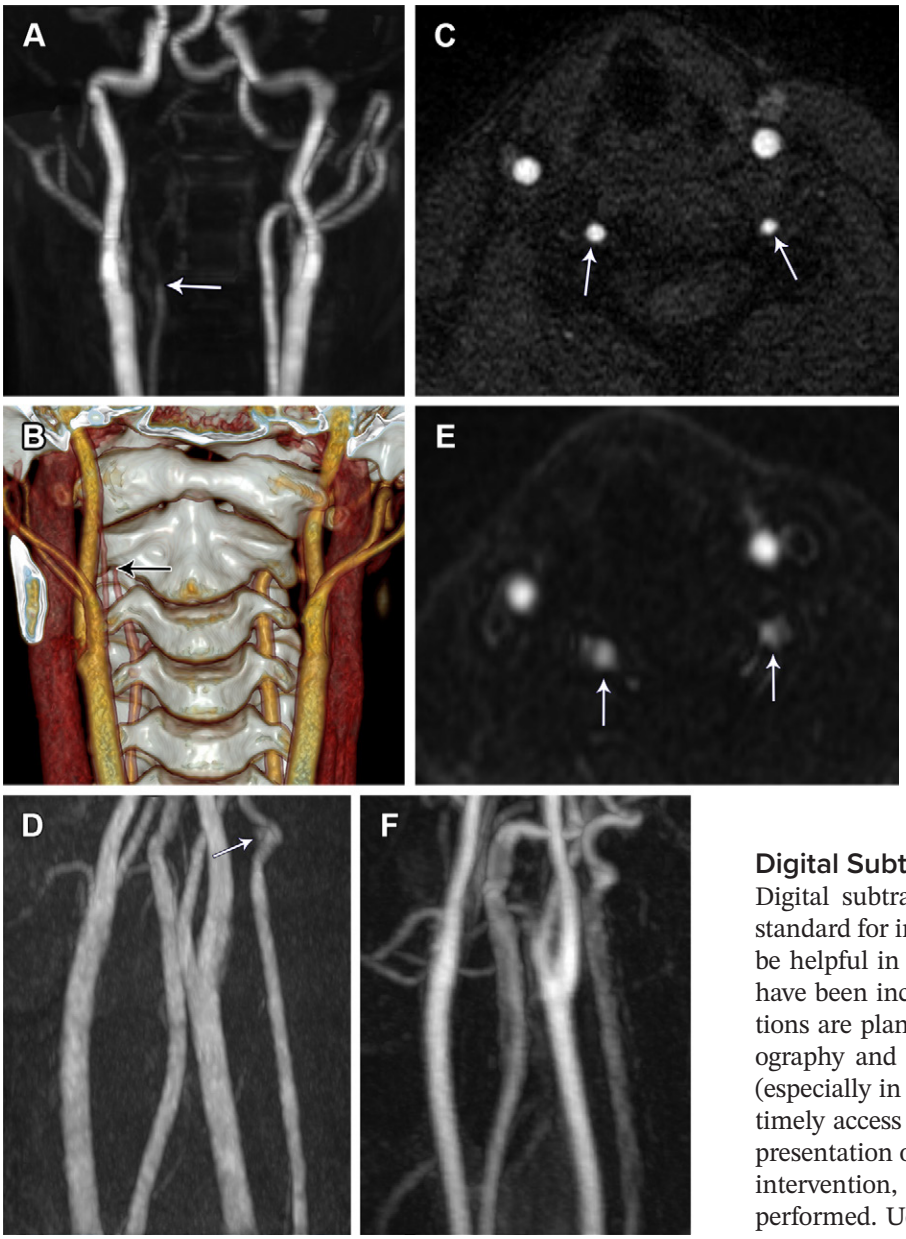

Figure 15. VAD in two children. The advantages and disadvantages of TOF MR angiography and contrast-enhanced imaging (CT angiography in case 1 [**A, B**]; contrast-enhanced MR angiography in case 2 [**C–F**]) in the assessment of VAD are highlighted. **(A, B)** Comparison of a coronal 2D TOF MIP MR angiogram **(A)**, showing occlusion of the right vertebral artery (arrow in **A**), with an anterior volume-rendered CT angiogram **(B)** in a 10-year-old girl with headache, nausea, neck pain, and right arm weakness (case 1) shows that the nonenhanced TOF MR angiogram **(A)** inaccurately characterized the level of occlusion, which was more distal at the C2 vertebral body level (arrow in **B**), due to slow flow proximal to the obstruction. **(C–F)** In a 12-year-old girl who presented with headache, visual disturbance, and tongue and mouth numbness (case 2), axial 3D TOF MR angiography was superior to contrast-enhanced MR angiography due to venous contamination on the contrast-enhanced MR angiogram. The nonenhanced axial **(C)** and sagittal oblique MIP **(D)** 3D TOF MR angiographic images of the vertebral arteries (arrows in **C**) had higher spatial resolution and better depicted a left vertebral artery pseudoaneurysm (arrow in **D**), compared with the contrast-enhanced axial **(E)** and sagittal oblique MIP **(F)** MR angiographic images. The pseudoaneurysm is obscured by the periarterial venous plexus on the MIP MR angiographic image **(F)**. 3D TOF MR angiography and contrast-enhanced CT or MR angiography may be complementary studies.

a T1-weighted 2D fat-saturated sequence. 2D TSE double–inversion-recovery (black-blood) imaging also provides better suppression of intraluminal signal than does 2D T1-weighted TSE fat-saturated imaging and may be useful if it is targeted to an area of interest (such as the proximal V3 segment) (Fig 16B). If used, the sequence ideally should be performed with a section thickness of less than 3 mm to best delineate the typically short segment of arterial involvement. However, z-axis spatial resolution may be inadequate, and a limited number of sections per repetition time may result in a long acquisition time.

Overall, the diagnosis of VAD with MR angiography remains challenging and insensitive at many institutions and has been shown to be less reliable than the diagnosis of this abnormality with digital subtraction angiography (with greater comparability in diagnosing basilar artery dissection) (12,13).

Digital Subtraction Angiography

Digital subtraction angiography is considered the reference standard for imaging cervical arterial dissection (14,32). It may be helpful in cases in which cross-sectional imaging findings have been inconclusive or endovascular therapeutic interventions are planned. However, given the usefulness of CT angiography and MR angiography, the risks of iatrogenic injury (especially in the acute period), and in some cases the lack of timely access to an experienced pediatric angiographer or the presentation of the patient outside the therapeutic window for intervention, digital subtraction angiography is infrequently performed. Uohara et al (3) noted that the use of digital subtraction angiography rarely changes decisions regarding antithrombotic therapy; both suspected and confirmed dissections are addressed with the same treatment. When evaluation for position-dependent dynamic vertebral artery compression is needed, CT angiography, which shows osseous abnormalities to an advantage, and digital subtraction angiography with dynamic maneuvers may be complementary (Fig 17).

Osseous Variants and Abnormalities, Dynamic Arterial Compression, and VAD

Rotational vertebral artery syndrome, or bow hunter syndrome, is defined as symptomatic vertebral arterial insufficiency related to physiologic head rotation. The term *bow hunter syndrome* has been misapplied as a synonym for dynamic vertebral artery compression (37). Although the symptoms are usually transient and self-limited in adults, this syndrome has been associated with VAD and stroke in children. Vertebral artery compression with head rotation is believed to cause repetitive microtrauma, recurrent vessel injury, and

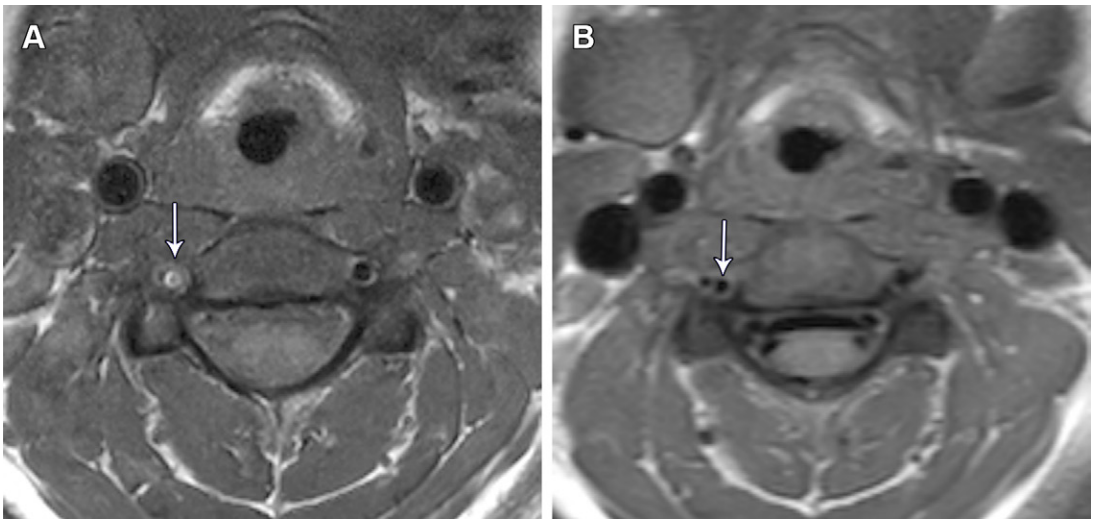

Figure 16. Slow flow in the right vertebral artery due to downstream occlusion in an 8-year-old boy. There was occlusion at the C2 level and thromboembolism within the right V4 segment (not pictured). **(A)** Axial T1-weighted TSE MR image shows increased signal intensity (arrow) in the right V2 vertebral artery segment due to slow flow, which may be confused with mural thrombus. High intravascular signal intensity on T1-weighted MR images is often due to slow flow rather than mural thrombus. **(B)** Axial double–inversion-recovery (T1-weighted black-blood) MR image shows a preserved flow void (arrow) without signs of thrombosis.

Figure 17. Multiple posterior circulation infarcts of varying age and VAD in a 10-year-old boy. This case demonstrates how CT angiography with dynamic maneuvers can help illustrate the relationship between bone anomalies and VAD, complementing catheter angiography. **(A)** Diffusion-weighted MRI on day 0 shows acute infarcts (arrows) of the right fusiform gyrus and midbrain. **(B)** Diffusion-weighted MR image on day 18 shows a new acute infarct (arrow) in the right thalamus. **(C)** Volume-rendered CT angiogram obtained with the patient's head in neutral position shows an anomalous bone protuberance (long arrow) of the right occipital condyle, in close proximity to the V3 segment of the right vertebral artery (short arrow). Digital subtraction angiography (not shown) showed no evidence of dynamic compression with head-turning maneuvers. **(D)** Volume-rendered CT angiogram with the patient's head tilted toward the left shoulder shows possible compression of the distal V3 segment (short arrow) between the anomalous protuberance superiorly and the C1 vertebra posterior arch inferiorly (long arrows). **(E)** 3D TOF MIP MR angiogram on day 319 shows a new pseudoaneurysm (arrow) at the same location.

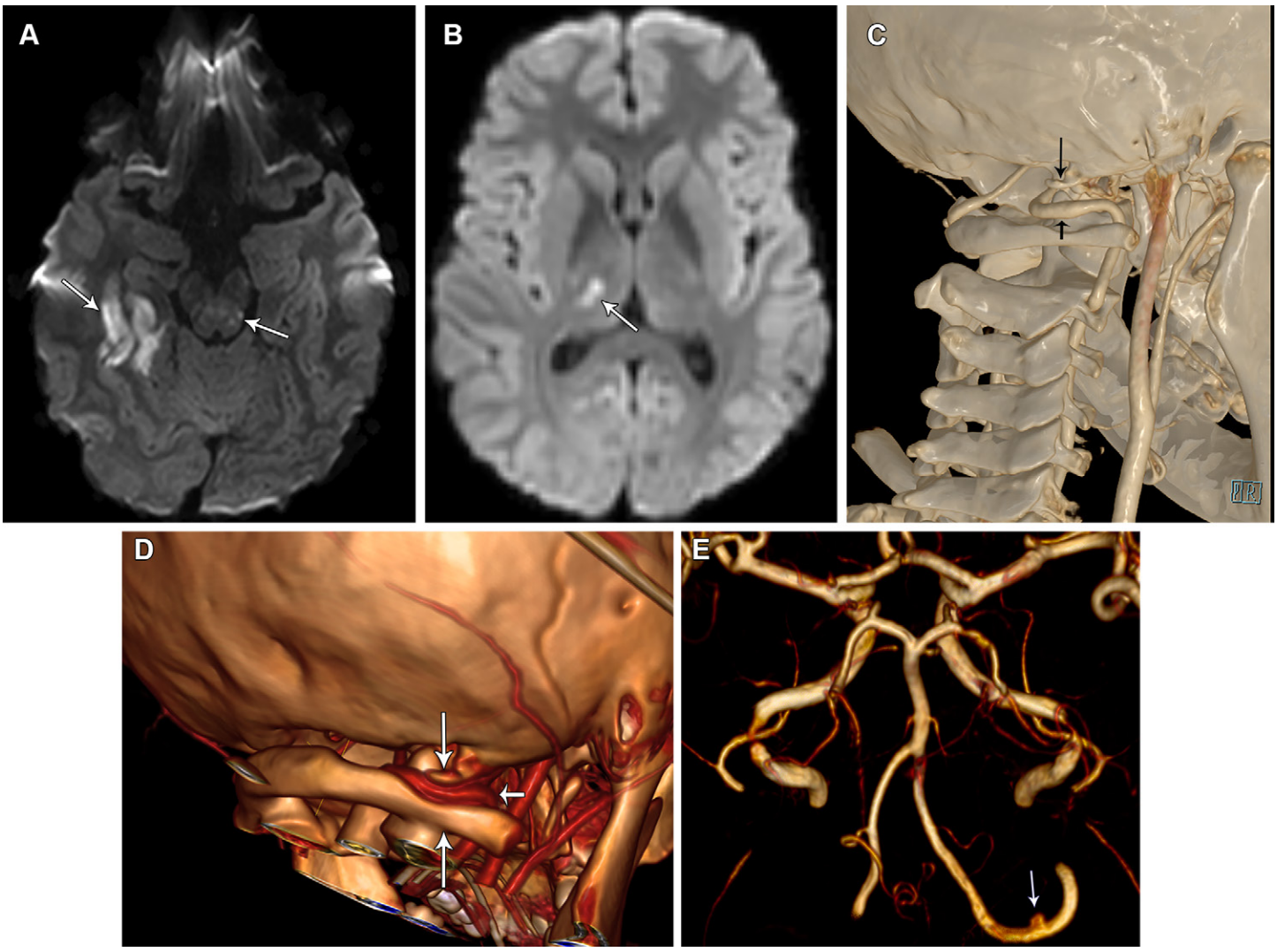

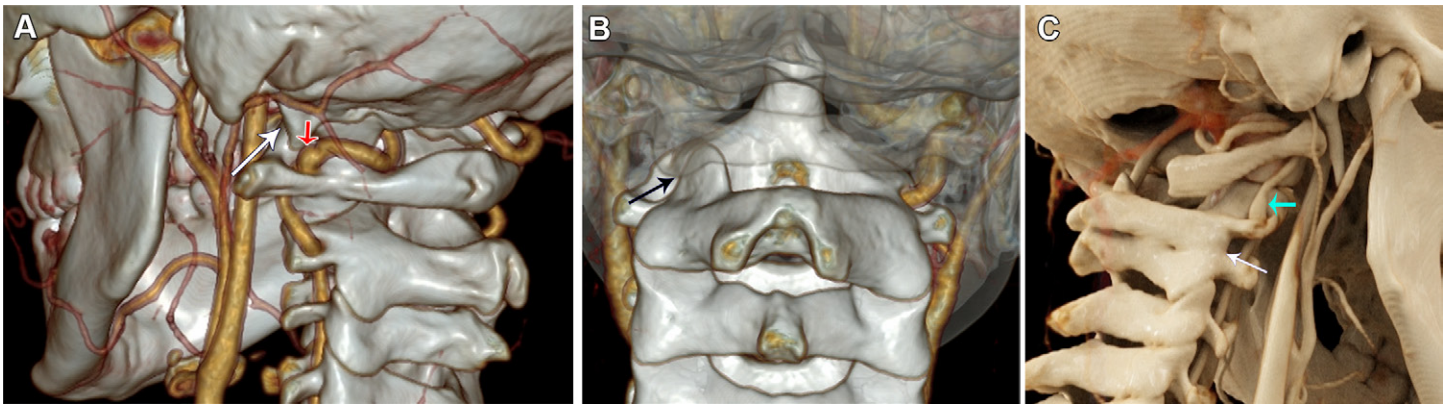

Figure 18. Anatomic variants believed to predispose to VAD in three children. **(A)** Left posterior oblique volume-rendered CT angiogram in a 16-year-old boy shows an anomalous occipital protuberance (white arrow) near a small left vertebral artery pseudoaneurysm (red arrow). This dissection atypically involves the distal horizontal V3 segment rather than the much more commonly involved proximal V3 segment. **(B)** Posterior volume-rendered CT angiogram in a 12-year-old girl shows an accessory left C1-C2 facet joint (arrow) adjacent to the C2 transverse foramen. The left vertebral artery was occluded at the V2 level. This anomaly may alter atlantoaxial mechanics and predispose to vertebral arteriopathy. **(C)** Right posterior oblique volume-rendered CT angiogram in a 10-year-old girl with Klippel-Feil syndrome and VAD shows C2-C3 interbody fusion, with asymmetric fusion of the posterior elements (white arrow). An incomplete posterior arch of C1 is also present. A right vertebral artery pseudoaneurysm (green arrow) is observed, and vertebral artery occlusion (not shown) was seen at follow-up imaging performed on day 57 after presentation.

Table 3: Osseous Variants that May Predispose to VAD

Paracondylar protuberance
Anomalous ossification of the C1 vertebra
Congenital arcuate foramen
Os odontoideum with cervical instability
Odontoid aplasia
Klippel-Feil anomaly
Accessory C1-C2 facet joint
C1 anterior arch anomaly
Lateral translocation of C1 vertebra, resulting in contact between the proximal V3 segment and C1 inferior facet

impaired arterial healing in some patients (14). The most common site of arterial compression with a head-turning maneuver is at the C1-C2 level. A high proportion of affected patients show evidence of dynamic compression during provocative angiography with head turning (24,37,49). However, dynamic compression may also be seen in patients without VAD (24,37).

Patients with signs of dynamic compression and VAD may have osseous anomalies, a soft-tissue abnormality (eg, ruptured atlantoaxial bursa or joint capsule, connective tissue scarring, fibrous band), atlantoaxial rotatory subluxation, or C1-C2 hypermobility (24,31,37,50). Without osseous anomalies, V3 vertebral artery narrowing is typically seen during contralateral head turning (31). Due to the high likelihood of associated dynamic compression, rotational digital subtraction angiography (after the acute period [discussed earlier in the "Digital Subtraction Angiography" section]) should be considered in patients with V3 VAD, even without a compressing extrinsic lesion being visible on CT or MR images. Pirozzi Chiusa et al (51) suggested that lateral head tilt rather than rotation may be implicated in patients with occipital osseous anomalies (eg, paracondylar bone spur) and distal V3 segment VAD. In patients with this finding, rotational angiography results may be negative.

Osseous anomalies or variants (Fig 18) may predispose pediatric patients to VAD by directly contacting the vertebral artery or by altering cervical biomechanics. The prevalence of clinically significant osseous variants may be underestimated owing to the infrequent use of CT as part of the imaging workup in some series (2). A list of these variants is provided in Table 3. The relationship between some osseous anomalies (including those not near the V3 vertebral segment) and VAD is unclear (Fig S5) (51,52).

Volume-rendered CT angiography is the best imaging technique for characterization of osseous anomalies and their relationships with the injured vertebral arterial segment. The role of provocative angiography in patients with osseous anomalies is controversial. However, the pathogenic significance of some osseous anomalies might be clarified with dynamic angiography.

The risk of PCAIS recurrence in patients with VAD may be especially high when there are mechanical predisposing factors such as osseous anatomic variants or cervical instability. Rotational VAD in children with adjacent osseous or soft-tissue abnormalities, or during neck rotation, is described in two case series. In one series (31), eight of 10 patients with VAD, PCAIS, and rotational vertebral arteriopathy experienced recurrent PCAIS, and five of 10 patients experienced multiple recurrences despite undergoing antithrombotic therapy. In an earlier series (37), six of seven boys with V3 segment VAD were found to have dynamic V3 compression at provocative digital subtraction angiography—either at initial imaging or at follow-up imaging performed for symptoms of transient ischemic attack.

In patients with predisposing extrinsic abnormalities that increase their risk for recurrent stroke, proposed adjuncts to pharmacologic treatment include temporary cervical immobilization, cervical spinal decompression and/or fusion, and endovascular stent placement or occlusion (22,24,31,51). However, the optimal management remains unclear in these rare and difficult cases.

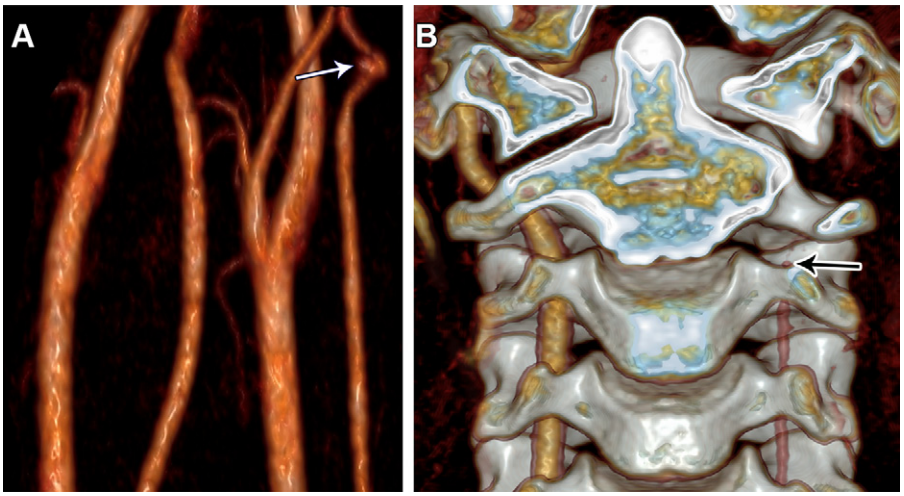

Figure 19. Left vertebral artery pseudoaneurysm that progressed to occlusion in a 12-year-old girl. **(A)** Oblique 3D volume-rendered TOF MR angiogram on day 0 shows a saccular pseudoaneurysm (arrow) in the left V3 segment, with preserved flow-related enhancement proximally. **(B)** Follow-up coronal volume-rendered CT angiogram on day 82 shows a new occlusion (arrow) near the V2-V3 junction and small caliber of the left vertebral artery.

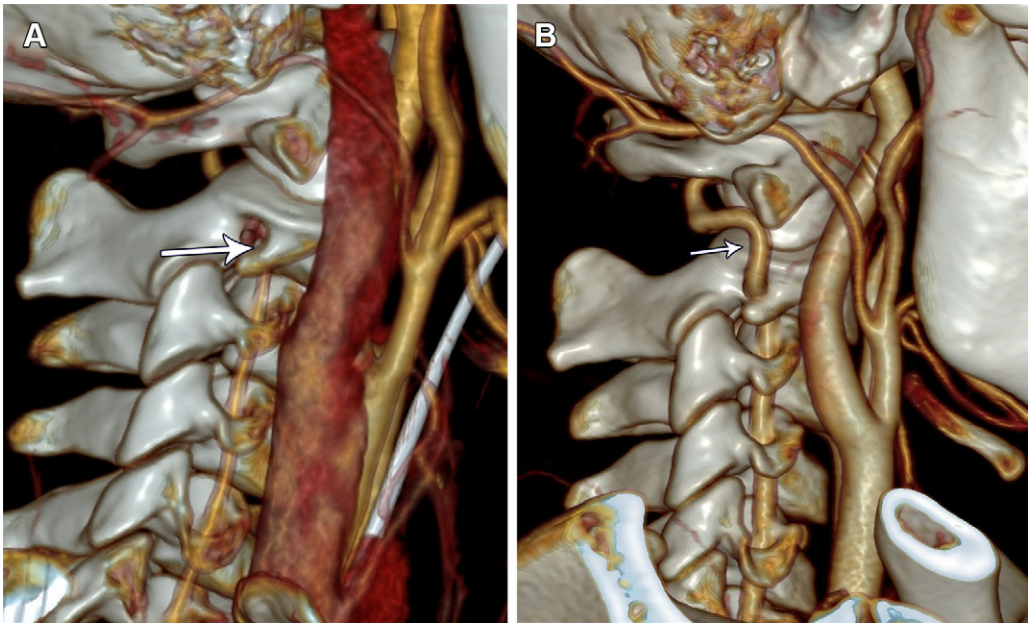

Figure 20. Right vertebral arterial occlusion, which was resolved at follow-up imaging, in an 8-year-old boy. **(A)** Right lateral volume-rendered CT angiogram on day 3 after clinical presentation shows occlusion (arrow) of the right vertebral artery at the C2 level. **(B)** Follow-up right lateral volume-rendered CT angiogram on day 410 shows a normal appearance of the right vertebral artery (arrow).

Role of Follow-up Imaging in VAD

The natural history of VAD has clinical implications for the timing and frequency of follow-up imaging. Cervical arterial dissection, especially posterior circulation dissection, can change over time. Nearly 50% of vessel abnormalities progress within the first year, and some arterial abnormalities may be detected only at follow-up (Fig 19) (2,10,13). Therefore, serial imaging, beginning at 3 months after initial clinical presentation and at intervals for at least 12 months, has been recommended. The goals for follow-up imaging are to detect new asymptomatic infarcts, monitor for vessel healing or improvement (Fig 20), and assess for pseudoaneurysms, which may be evident only at follow-up imaging and may indicate a higher risk for stroke recurrence (2,14). Bilateral VAD is not rare, although it is less common in children than in adults, and it may be first detected at follow-up (Fig S6) (21). Even if the arteries are patent at initial imaging, vascular narrowing or occlusion (which may be a manifestation of appropriate healing) is commonly identified at long-term follow-up (21).

Conclusion

The diagnosis of pediatric PCAIS is often challenging and sometimes delayed. Multifocal infarcts of varying age (including chronic infarcts) are commonly seen at the time of initial imaging. PCAIS and/or findings of posterior circulation arteriopathy (particularly abrupt arterial occlusions) should prompt optimized imaging assessment for VAD, preferably with 3D TOF MR angiography or with CT angiography of the cervical vessels. VAD may be difficult to identify or not visible at initial imaging (even digital subtraction angiography), and it may first become apparent on follow-up images. Pediatric VAD is most common at the

V2-V3 junction and proximal V3 segment. CT angiography is useful for depicting osseous variants and anomalies that predispose to VAD by impinging on the vertebral artery or altering biomechanics. Provocative maneuvers performed at digital subtraction angiography or CT angiography may reveal dynamic arterial compression. For children, anticoagulation rather than antiplatelet therapy may need to be considered owing to the increased risk for stroke recurrence compared with this risk in adults, with surgical management considered in select cases.

Author affiliations.—From the Departments of Radiology (S.B.L., M.B., K.R.), Neurosurgery and Pediatrics (A.R.), and Pediatrics-Child Neurology (B.P.), Children's Healthcare of Atlanta, Emory University, Atlanta, GA; and Departments of Radiology (A.S., S.P.) and Pediatrics (L.C.J.), Vanderbilt University Medical Center, Monroe Carell Jr Children's Hospital, 2200 Children's Way, Nashville, TN 37323. Recipient of a Certificate of Merit award for an education exhibit at the 2022 RSNA Annual Meeting. Received April 24, 2023; revision requested May 31 and received June 23; accepted July 10. **Address correspondence to** A.S. (email: *asha.sarma@vumc.org*).

Disclosures of conflicts of interest.—**S.P.** Noncompensated member of advisory board for Sectra PACS. **B.P.** Emory University travel account and appointment benefits; registration for American Heart Association International Stroke Conference waived for moderating session.

References

1. Goeggel Simonetti B, Rafay MF, Chung M, et al; IPSS Study Group. Comparative study of posterior and anterior circulation stroke in childhood: Results from the International Pediatric Stroke Study. Neurology 2020;94(4):e337–e344.
2. McCrea N, Saunders D, Bagkeris E, Chitre M, Ganesan V. Diagnosis of vertebral artery dissection in childhood posterior circulation arterial ischaemic stroke. Dev Med Child Neurol 2016;58(1):63–69.
3. Uohara MY, Beslow LA, Billinghurst L, et al. Incidence of Recurrence in Posterior Circulation Childhood Arterial Ischemic Stroke. JAMA Neurol 2017;74(3):316–323.
4. Rafay MF, Shapiro KA, Surmava A-M, et al; International Pediatric Stroke Study (IPSS) Group. Spectrum of cerebral arteriopathies in children with arterial ischemic stroke. Neurology 2020;94(23):e2479–e2490.
5. Wintermark M, Hills NK, DeVeber GA, et al; VIPS Investigators. Clinical and Imaging Characteristics of Arteriopathy Subtypes in Children with Arterial Ischemic Stroke: Results of the VIPS Study. AJNR Am J Neuroradiol 2017;38(11):2172–2179.
6. Markus HS, Levi C, King A, Madigan J, Norris J; Cervical Artery Dissection in Stroke Study (CADISS) Investigators. Antiplatelet Therapy vs Anticoagulation Therapy in Cervical Artery Dissection: The Cervical Artery Dissection in Stroke Study (CADISS) Randomized Clinical Trial Final Results. JAMA Neurol 2019;76(6):657–664.
7. Ganesan V, Cox TC, Gunny R. Abnormalities of cervical arteries in children with arterial ischemic stroke. Neurology 2011;76(2):166–171.
8. Bernard TJ, Manco-Johnson MJ, Lo W, et al. Towards a consensus-based classification of childhood arterial ischemic stroke. Stroke 2012;43(2):371–377.
9. Nash M, Rafay MF. Craniocervical Arterial Dissection in Children: Pathophysiology and Management. Pediatr Neurol 2019;95:9–18.
10. Mackay MT, Prabhu SP, Coleman L. Childhood posterior circulation arterial ischemic stroke. Stroke 2010;41(10):2201–2209.
11. Rambaud T, Legris N, Bejot Y, et al. Acute ischemic stroke in adolescents. Neurology 2020;94(2):e158–e169.
12. Rollins N, Pride GL, Plumb PA, Dowling MM. Brainstem strokes in children: an 11-year series from a tertiary pediatric center. Pediatr Neurol 2013;49(6):458–464.
13. Tan MA, Armstrong D, MacGregor DL, Kirton A. Late complications of vertebral artery dissection in children: pseudoaneurysm, thrombosis, and recurrent stroke. J Child Neurol 2009;24(3):354–360.
14. Ferriero DM, Fullerton HJ, Bernard TJ, et al; American Heart Association Stroke Council and Council on Cardiovascular and Stroke Nursing. Management of Stroke in Neonates and Children: A Scientific Statement From the American Heart Association/American Stroke Association. Stroke 2019;50(3):e51–e96.
15. Medley TL, Miteff C, Andrews I, et al. Australian Clinical Consensus Guideline: The Diagnosis and Acute Management of Childhood Stroke. Int J Stroke 2019;14(1):94–106.
16. Kleindorfer DO, Towfighi A, Chaturvedi S, et al. 2021 Guideline for the Prevention of Stroke in Patients With Stroke and Transient Ischemic Attack: A Guideline From the American Heart Association/American Stroke Association. Stroke 2021;52(7):e364–e467. [Published correction appears in Stroke 2021;52(7):e483-e484.]
17. Fullerton HJ, Johnston SC, Smith WS. Arterial dissection and stroke in children. Neurology 2001;57(7):1155–1160.
18. Völker W, Dittrich R, Grewe S, et al. The outer arterial wall layers are primarily affected in spontaneous cervical artery dissection. Neurology 2011;76(17):1463–1471.
19. Fink M, Slavova N, Grunt S, et al. Posterior Arterial Ischemic Stroke in Childhood. Stroke 2019;50(9):2329–2335.
20. Songsaeng D, Srivatanakul K, Krings T, Geibprasert S, Ozanne A, Lasjaunias P. Symptomatic spontaneous vertebrobasilar dissections in children: review of 29 consecutive cases. J Neurosurg Pediatr 2010;6(3):233–243.
21. Simonnet H, Deiva K, Bellesme C, et al. Extracranial vertebral artery dissection in children: natural history and management. Neuroradiology 2015;57(7):729–738.
22. Ritchey Z, Bernard TJ, Fenton LZ, et al. Stroke Recurrence in Children with Vertebral Artery Dissecting Aneurysm. AJNR Am J Neuroradiol 2022;43(6):913–918.
23. Carey S, Wrogemann J, Booth FA, Rafay MF. Epidemiology, Clinical Presentation, and Prognosis of Posterior Circulation Ischemic Stroke in Children. Pediatr Neurol 2017;74:41–50.
24. Braga BP, Sillero R, Pereira RM, et al. Dynamic compression in vertebral artery dissection in children: apropos of a new protocol. Childs Nerv Syst 2021;37(4):1285–1293.
25. Weber CD, Lefering R, Weber MS, et al; TraumaRegister DGU. Predictors for Pediatric Blunt Cerebrovascular Injury (BCVI): An International Multicenter Analysis. World J Surg 2019;43(9):2337–2347.
26. Kadom N, Palasis S, Pruthi S, et al; Expert Panel on Pediatric Imaging. ACR Appropriateness Criteria: Suspected Spine Trauma—Child. J Am Coll Radiol 2019;16(5 5S):S286–S299.
27. Engelter ST, Traenka C, Gensicke H, et al; TREAT-CAD investigators. Aspirin versus anticoagulation in cervical artery dissection (TREAT-CAD): an open-label, randomised, non-inferiority trial. Lancet Neurol 2021;20(5):341–350.
28. Gordon WR, Edgell RC. Neurointervention in the Medical Specialties: A Comprehensive Guide. Curr Clin Neurology, 2022; 9–21.
29. Böhmer M, Niederstadt T, Heindel W, et al. Impact of Childhood Arterial Ischemic Stroke Standardized Classification and Diagnostic Evaluation Classification on Further Course of Arteriopathy and Recurrence of Childhood Stroke. Stroke 2019;50(1):83–87.
30. Pandey S, Hakky M, Kwak E, Jara H, Geyer CA, Erbay SH. Application of basic principles of physics to head and neck MR angiography: troubleshooting for artifacts. RadioGraphics 2013;33(3):E113–E123.
31. Fox CK, Fullerton HJ, Hetts SW, et al. Single-center series of boys with recurrent strokes and rotational vertebral arteriopathy. Neurology 2020;95(13):e1830–e1834.
32. Hanning U, Sporns PB, Schmiedel M, et al. CT versus MR Techniques in the Detection of Cervical Artery Dissection. J Neuroimaging 2017;27(6):607–612.
33. Robertson RL, Palasis S, Rivkin MJ, et al; Expert Panel on Pediatric Imaging. ACR Appropriateness Criteria: Cerebrovascular Disease—Child. J Am Coll Radiol 2020;17(5 5S):S36–S54.
34. Bernard TJ, Beslow LA, Manco-Johnson MJ, et al. Inter-Rater Reliability of the CASCADE Criteria: Challenges in Classifying Arteriopathies. Stroke 2016;47(10):2443–2449.
35. Zuccoli G, Fitz C, Greene S, et al. Imaging Review of Common and Rare Causes of Stroke in Children. Top Magn Reson Imaging 2018;27(6):463–477.
36. ACR-ASNR-SPR Practice Parameter for the Performance and Interpretation of Cervicocerebral Computed Tomography Angiography (CTA). American College of Radiology. https://www.acr.org/-/media/ACR/Files/Practice-Parameters/CervicoCerebralCTA.pdf. Revised 2020. Accessed April 24, 2023.
37. Rollins N, Braga B, Hogge A, Beavers S, Dowling M. Dynamic Arterial Compression in Pediatric Vertebral Arterial Dissection. Stroke 2017;48(4):1070–1073.
38. Symons R, Reich DS, Bagheri M, et al. Photon-Counting Computed Tomography for Vascular Imaging of the Head and Neck: First In Vivo Human Results. Invest Radiol 2018;53(3):135–142.
39. Schellinger PD, Bryan RN, Caplan LR, et al. Evidence-based guideline: the role of diffusion and perfusion MRI for the diagnosis of acute ischemic stroke—report of the Therapeutics and Technology Assessment Subcommittee of the American Academy of Neurology. Neurology 2010;75(2):177–185. [Published correction appears in Neurology 2010;75(10):938.]
40. Jaimes C, Robson CD, Machado-Rivas F, et al. Success of Nonsedated Neuroradiologic MRI in Children 1-7 Years Old. AJR Am J Roentgenol 2021;216(5):1370–1377.

41. Wharton JD, Barry MM, Lee CA, Massey K, Ladner TR, Jordan LC. Pediatric Acute Stroke Protocol Implementation and Utilization Over 7 Years. J Pediatr 2020;220:214–220.e1.
42. Oelerich M, Stögbauer F, Kurlemann G, Schul C, Schuierer G. Craniocervical artery dissection: MR imaging and MR angiographic findings. Eur Radiol 1999;9(7):1385–1391.
43. Arnold M, Bousser MG, Fahrni G, et al. Vertebral artery dissection: presenting findings and predictors of outcome. Stroke 2006;37(10):2499–2503.
44. Vertinsky AT, Schwartz NE, Fischbein NJ, Rosenberg J, Albers GW, Zaharchuk G. Comparison of multidetector CT angiography and MR imaging of cervical artery dissection. AJNR Am J Neuroradiol 2008;29(9):1753–1760.
45. Edjlali M, Roca P, Rabrait C, Naggara O, Oppenheim C. 3D fast spin-echo T1 black-blood imaging for the diagnosis of cervical artery dissection. AJNR Am J Neuroradiol 2013;34(9):E103–E106.
46. Nguyen Bui L, Brant-Zawadzki M, Verghese P, Gillan G. Magnetic resonance angiography of cervicocranial dissection. Stroke 1993;24(1):126–131.
47. Cuvinciuc V, Viallon M, Momjian-Mayor I, et al. 3D fat-saturated T1 SPACE sequence for the diagnosis of cervical artery dissection. Neuroradiology 2013;55(5):595–602.
48. McNally JS, Hinckley PJ, Sakata A, et al. Magnetic Resonance Imaging and Clinical Factors Associated With Ischemic Stroke in Patients Suspected of Cervical Artery Dissection. Stroke 2018;49(10):2337–2344.
49. Anene-Maidoh TI, Vega RA, Fautheree GL, Reavey-Cantwell JF. An unusual case of pediatric bow hunter's stroke. Surg Neurol Int 2013;4(1):148.
50. Hu Y, Du J, Liu Z, Wu H, Ding J, Jian F. Vertebral artery dissection caused by atlantoaxial dislocation: a case report and review of literature. Childs Nerv Syst 2019;35(1):187–190.
51. Pirozzi Chiusa CG, Pinto MR, Ferrario A, Ruella M, Routaboul C. Clinical response to surgical decompression in atypical pediatric bow hunter's syndrome suggesting alternative pathophysiology: case report. Childs Nerv Syst 2022;38(11):2199–2203.
52. Greiner HM, Abruzzo TA, Kabbouche M, Leach JL, Zuccarello M. Rotational vertebral artery occlusion in a child with multiple strokes: a case-based update. Childs Nerv Syst 2010;26(12):1669–1674.